# A New Family of Generalized Distributions, with Applications and Benchmarking against Machine Learning Models

Bassant Elkalzah[1,2], Emmanuel E. Oguadimma[3], Victory C. Obieke[3], Chinonso Michael Eze[4,*], Okechukwu J. Obulezi[5] and Mohammed Elgarhy[6,7,8]

[1]*Department of Mathematics and Statistics, College of Science, Imam Mohammad Ibn Saud Islamic University (IMSIU), Riyadh, 11432, Saudi Arabia*

[2]*Department of Statistics, Mathematics and Insurance, Faculty of Business, Alexandria University, Alexandria, 21526, Egypt*

[3]*Department of Mathematics, Oregon State University, Corvallis, OR 97331, USA*

[4]*Department of Statistics, Faculty of Physical Sciences, University of Nigeria, Nsukka, Nigeria*

[5]*Department of Statistics, Faculty of Physical Sciences, Nnamdi Azikiwe University, P.O. Box 5025 Awka, Nigeria*

[6]*Faculty of Computers and Information Systems, Egyptian Chinese University, Nasr City, Egypt*

[7]*Department of Basic Sciences, Higher Institute of Administrative Sciences, Belbeis, AlSharkia, Egypt*

[8]*Department of Computer Engineering, Biruni University, 34010, Istanbul, Turkey*

**Abstract:** In this study, we introduce a new family of generalized distributions using the Lomax tangent generalized transformation. We derive the general formulas for its cumulative distribution function (CDF) and probability density function (PDF). As a specific sub-model, we construct the new generalized Lomax tangent transformed exponential (NGLTGE) distribution by using the exponential distribution as the baseline. We investigate the model's key mathematical properties and conduct a Monte Carlo simulation, which confirms that the estimators exhibit good asymptotic behavior. A group acceptance sampling plan is also designed to demonstrate its utility in quality control. The NGLTGE model is then applied to real-world datasets from cryptocurrency, COVID-19, and breast cancer, where it consistently provides a superior statistical fit compared to related distributions. Finally, we apply the NGLTGE distribution within a machine learning framework using a PyTorch maximum likelihood estimation. The model's predictive performance is found to be competitive with, and in some cases superior to, state-of-the-art machine learning density estimators like the Log-Gaussian Mixture Model (Log-GMM) and Masked Autoregressive Flow (MAF), especially for data with heavy tails. This work positions the NGLTGE distribution as a valuable, interpretable, and scalable model for both classic statistical and modern data science applications.

**Keywords:** Generalized distributions, Lomax tangent generalized family, Monte Carlo Simulation, Log-Gaussian Mixture Model, Masked Autoregressive Flow.

## 1. INTRODUCTION

Choosing the right statistical distribution for a dataset is a critical step, as there is often no single, obvious choice. A common, but not always objective, method involves testing multiple distributions and selecting the one that best fits the data, but a more efficient approach is to use a general family of distributions, such as Pearson's, that can be adjusted to fit a wide range of data [1]. Generalization is a common and fascinating approach to designing new families of distributions. In the end, the structural cum functional form of the based distribution is altered. This often leads to a more robust model with better goodness-of-fit, parameter estimates with minimum standard errors, and tractable characteristics. The new families fashioned this way are known for being able to capture intricate properties of datasets that the parent distributions could not capture. Such generalizations include the Kumaraswamy generalized family by [2], the log-logistic tangent generalized family by [3], new sine family of generalized distributions by [4], new two-parameter mixture family of generalized distributions by [5], new Kumaraswamy Kumaraswamy family of generalized distributions by [6], new flexible generalized family by, new generalized Weibull family by [7], weighted general family by [8], a new generalized normal family by [9], new power generalized Weibull family by [10], odd generalized exponential family of distributions by [11], generalized gamma family by [12], generalized symmetric family by [13], generalized transmuted family by [14], novel generalized family by [15]. Other readings include [16-25] to mention a few.

[26] was the first to introduce a new family of generalized distributions using the transformation of the cdf of another family of distributions. That is, the cdf of alpha power family. [27] proposed a new family of generalized distributions based on the logistic x

*Address correspondence to this author at the Department of Statistics, Faculty of Physical Sciences, University of Nigeria, Nsukka, Nigeria;
E-mail: chinonso.eze@unn.edu.ng

transformation. In the present study, we design a new family of generalized distributions based on the lomax tangent generalized transformation. Let $X$ be a nonnegative real-valued random variable that is lomax tangent generalized distributed [28], the cumulative distribution function (CDF) is given in Eq. (1.1) as;

$$G(x;s,k,\zeta)=1-\left[1+\frac{\tan\left(\frac{\pi}{2}F(x;\zeta)\right)}{s}\right]^{-k};\quad x>0,\quad s,k>0,\quad (1.1)$$

where $F(x;\zeta)$ is any continuous baseline distribution. Taking $F(x;\zeta)$ as the subject in Eq. (1.1), we have

$$F(x;s,k,\zeta)=\frac{2}{\pi}\arctan\left\{s\left[1-G(x;\zeta)\right]^{-\frac{1}{k}}-s\right\};\quad x>0,\quad s,k>0,\quad (1.2)$$

where $\zeta$ is the vector of parameters for the baseline distribution, now redesigned as $G(x;\zeta)$. Differentiating Eq. (1.2) produces the associated probability density function (PDF) given in Eq. (1.3) as;

$$f(x;s,k,\zeta)=\left(\frac{2s}{\pi k}\right)\frac{g(x;\zeta)\left[1-G(x;\zeta)\right]^{-\frac{1}{k}-1}}{1+\left\{s\left[1-G(x;\zeta)\right]^{-\frac{1}{k}}-s\right\}^2};\quad x>0,\quad s,k>0.\quad (1.3)$$

The quantile function is

$$Q(u)=G^{-1}\left(1-\left(\frac{\tan\left(\frac{\pi u}{2}\right)+s}{s}\right)^{-k}\right);\quad u\in(0,1).$$

The rationale for this work is multi-faceted, founded on the perennial problem of adequate modeling of complex and diverse data sets in economics, finance, and medical sciences. Most standard econometric models and statistical distributions can seldom explain the non-linear dynamics, heavy tails, and volatility of economic time series, financial returns like Bitcoin, and survival times from diseases like COVID-19 and breast cancer. The novel Lomax Tangent (LT) generalized transformation is specifically introduced to address this gap because its structure is hypothesized to provide enhanced flexibility: it leverages the Lomax generator for superior heavy-tail modeling (allowing for greater kurtosis control) and uses the tangent function for non-linear domain mapping and complex PDF shape generation. It is this need to create a uniform, robust, and extremely versatile probability distribution specifically the New Generalized Lomax Tangent Transformed Exponential (NGLTGE) distribution that can best account for these varied phenomena that this paper attempts to focus on. The work aims to demonstrate that this novel distribution not only achieves a better statistical fit compared to the classic rivals but is also a competitive parametric density estimator in a modern machine learning framework, thus combining classical statistics and recent data science. The ultimate aim is to develop a robust, interpretable, and scalable model that can be employed to address a wide range of real-world issues for which existing models do not work.

In the remaining sections, the NGLTGE model is constructed in Section 2. Its structural properties are examined in Section 3 while the parameters are estimated in Section‘4. In Section 5, a comprehensive simulation study is carried out to determine the behaviour of the estimators in the presence of small and large sample sizes. In Section 6 a group acceptance sampling plan is designed to support the utility of the NGLTGE in the assessment of quality control. Numerical analysis is presented in Section 7 with the extension of the proposed NGLTGE distribution to a broader machine learning concept demonstrated in Section 8. The study is concluded in Section 9, which provides ideas for future research.

## 2. SUBMODEL: NGLTG-EXPONENTIAL (NGLTGE) DISTRIBUTION

The CDF and PDF of the exponential distribution with scale parameter $\theta$ are given as

$$G(x;\theta)=1-e^{-\theta x};\quad x>0,\quad \theta>0,\quad (2.1)$$

and

$$g(x;\theta)=\theta e^{-\theta x}.\quad (2.2)$$

Substituting Eqs. (2.1) and (2.2) in Eqs. (1.2) and (1.3) accordingly, we realized the CDF and PDF of the NGLTGE distribution, respectively given as

$$F(x;s,k,\theta)=\frac{2}{\pi}\arctan\left\{se^{\frac{\theta x}{k}}-s\right\};\quad x>0,\quad s,k,\theta>0,\quad (2.3)$$

and

$$f(x;s,k,\theta)=\frac{2s\theta e^{\frac{\theta x}{k}}}{\pi k\left(1+\left[se^{\frac{\theta x}{k}}-s\right]^2\right)};\quad x>0,\quad s,k,\theta>0.\quad (2.4)$$

The quantile function is expressed as

$$Q(u)=\frac{k}{\theta}\log\left\{1+\frac{1}{s}\tan\left(\frac{\pi u}{2}\right)\right\};\quad u\in(0,1).\quad (2.5)$$

Figure **1** represents plots of the PDF and hazard function of the proposed NGLTGE distribution. In panel 1, the curves exhibit diverse shapes, including

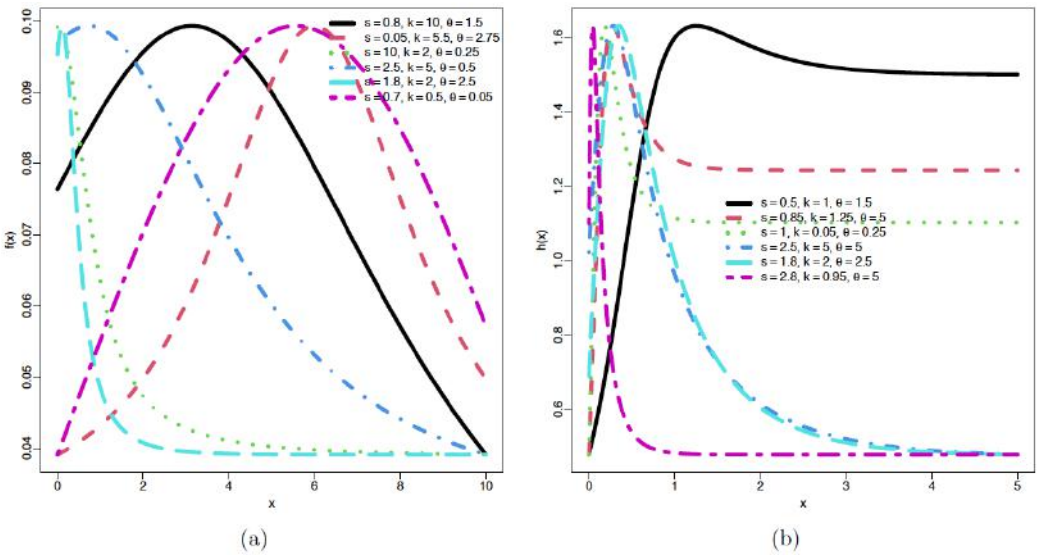


**Figure 1:** Plots of (**a**) pdf (**b**) hazard function for NGLTGE distribution.

unimodal, bimodal, and positively skewed forms, indicating the NGLTGE distribution's flexibility in modeling different data patterns. The varying peaks and tails of these curves suggest that the distribution can adapt to a wide range of real-world phenomena. In panel 2, the shapes are also varied, showing decreasing, increasing, and bathtub-shaped hazard rates. This diversity demonstrates the distribution's utility in reliability and survival analysis, where it can model different failure behaviors over time.

## 3. STRUCTURAL PROPERTIES

In this section, we develop the structural properties of the NGLTGE submodel.

### 3.1. Boundary Limits

**Proposition 1.1** For all $s,k,\theta>0$, and using the definition (2.3)

$$\lim_{x\downarrow 0}F(x;s,k,\theta)=0 \qquad \textit{and} \qquad \lim_{x\uparrow\infty}F(x;s,k,\theta)=1.$$

*Proof.* Define $g(x):=s(e^{\theta x/k}-1)$. Then (2.3) reads $F(x)=(2/\pi)\arctan(g(x))$.

*Limit at* $0$. Since $e^0=1$ and $\exp$ is continuous, $\lim_{x\downarrow 0}g(x)=0$. By continuity of $\arctan$ and $\arctan(0)=0$,

$$\lim_{x\downarrow 0}F(x)=\frac{2}{\pi}\arctan(\lim_{x\downarrow 0}g(x))=0.$$

For a quantitative bound, note the inequalities $\arctan y\le y$ for $y\ge 0$ and $e^u-1\le ue^u$ for $u\ge 0$; thus, for $x>0$,

$$0\le F(x)\le \frac{2}{\pi}g(x)=\frac{2s}{\pi}(e^{\theta x/k}-1)\le \frac{2s}{\pi}\frac{\theta x}{k}e^{\theta x/k}\xrightarrow[x\downarrow 0]{}0.$$

*Limit at* $+\infty$. Since $\theta/k>0$, $e^{\theta x/k}\to\infty$ and hence $g(x)\to\infty$ as $x\uparrow\infty$. Using $\lim_{y\to\infty}\arctan y=\pi/2$,

$$\lim_{x\uparrow\infty}F(x)=\frac{2}{\pi}\cdot\frac{\pi}{2}=1.$$

as desired.

**Corollary 1.1** For $x>0$, $0<F(x)<1$. Moreover, $\lim_{x\downarrow 0}F(x)=0$ and $\lim_{x\uparrow\infty}F(x)=1$. Thus $F$ maps $(0,\infty)$ into $(0,1)$, is right-continuous at $0$, and approaches $1$ at $+\infty$.

**Lemma 1.1** As $x\downarrow 0$,

$$F(x)=\frac{2s\theta}{\pi k}x+\mathcal{O}(x), \qquad f(0^+)=\frac{2s\theta}{\pi k}.$$

As $x\uparrow\infty$,

$$1-F(x)=\frac{2}{\pi}\frac{1}{se^{\theta x/k}}+\mathcal{O}(e^{-\theta x/k})=\frac{2}{\pi s}e^{-\theta x/k}+\mathcal{O}(e^{-\theta x/k}).$$

*Proof.* For $x\downarrow 0$, use $e^u=1+u+\mathcal{O}(u)$ and $\arctan y=y+\mathcal{O}(y)$ as $u,y\to 0$:

$$F(x)=\frac{2}{\pi}\arctan(s(e^{\theta x/k}-1))=\frac{2}{\pi}(s\frac{\theta}{k}x)+\mathcal{O}(x).$$

Differentiating (2.3) or evaluating (2.4) at $x=0$ yields $f(0^+)=\frac{2s\theta}{\pi k}$.

For $x \uparrow \infty$, write $F(x) = 1 - \frac{2}{\pi} arccot(g(x))$ and use $arccoty = y^{-1} + \mathcal{O}(y^{-1})$ as $y \to \infty$ to obtain

$$1 - F(x) = \frac{2}{\pi} \frac{1}{g(x)} + \mathcal{O}(g(x)^{-1}) = \frac{2}{\pi} \frac{1}{se^{\theta x/k} - s} + \mathcal{O}(e^{-\theta x/k}) = \frac{2}{\pi s} e^{-\theta x/k} + \mathcal{O}(e^{-\theta x/k}),$$

a tail estimate that will feed moment/tail-class results later.

### 3.2. Regularity

**Proposition 2.1** Consider (2.3)-(2.4). Then:

1. $F \in C^{\infty}((0,\infty))$. In particular, for every $x > 0$, $F'(x) = f(x)$.

2. For any $0 < a < b < \infty$, $F$ is absolutely continuous on $[a,b]$; with the extension at $0$, $F$ is absolutely continuous on every $[0,b]$ and

$$F(x) = \int_0^x f(t)dt \qquad (x > 0).$$

*Proof.* (i) On $(0,\infty)$, both $\exp$ and $\arctan$ are $C^{\infty}$, and compositions of $C^{\infty}$ functions are $C^{\infty}$, hence $F \in C^{\infty}((0,\infty))$. Writing $h(x) := se^{\theta x/k} - s$, the chain rule yields

$$F'(x) = \frac{2}{\pi} \frac{h'(x)}{1 + h(x)^2} = \frac{2}{\pi} \cdot \frac{1}{1 + (se^{\theta x/k} - s)^2} \cdot (se^{\theta x/k} \frac{\theta}{k}) = f(x).$$

(iii) On any compact subinterval $[a,b] \subset (0,\infty)$, $f$ is continuous, hence integrable, and the Fundamental Theorem of Calculus gives $F(x) = F(a) + \int_a^x f(t)dt$. Using the continuous extension $F(0) = 0$ and the fact that $f$ is bounded near $0$ (indeed $\lim_{x \downarrow 0} f(x) = \frac{2s\theta}{\pi k}$), we obtain $F(x) = \int_0^x f(t)dt$ for all $x > 0$. Thus $F$ is absolutely continuous on each $[0,b]$ and the stated integral representation holds.

**Corollary 2.1** For $s,k,\theta > 0$, one has $f(x) > 0$ for all $x > 0$, hence $F$ is strictly increasing on $(0,\infty)$. Consequently, the quantile function $Q(p) := F^{-1}(p)$ exists for every $p \in (0,1)$ and is continuous and strictly increasing in $p$.

*Proof.* Each factor in $f(x)$ is positive for $x > 0$, so $f(x) > 0$ and $F$ is strictly increasing. The inverse and its properties then follow from standard results for continuous strictly increasing functions on $(0,\infty)$ with limits $0$ and $1$ at the endpoints.

**Proposition 2.2** For each fixed $x > 0$,

$$\frac{\partial F}{\partial s}(x;s,k,\theta) > 0, \quad \frac{\partial F}{\partial \theta}(x;s,k,\theta) > 0, \quad \frac{\partial F}{\partial k}(x;s,k,\theta) < 0.$$

Hence, $F$ is strictly increasing in $s$ and $\theta$, and strictly decreasing in $k$

*Proof.* Differentiate (2.3) with respect to each parameter and result follows.

### 3.3. Survival Function

For an absolutely continuous CDF $F$, the survival function is defined by $S(x) = 1 - F(x)$. For the NGLTGE model (2.3), and for each $x > 0$ and $s,k,\theta > 0$, the closed form is derived as follows

$$S(x;s,k,\theta) = 1 - F(x;s,k,\theta) = 1 - \frac{2}{\pi} \arctan\left( se^{\frac{\theta x}{k}} - s \right) \tag{3.1}$$

**Lemma 3.1 (Alternative closed form)** For every $x > 0$ and $s,k,\theta > 0$,

$$S(x;s,k,\theta) = \frac{2}{\pi} \arctan\left( \frac{1}{se^{\frac{\theta x}{k}} - s} \right).$$

*Proof.* For $x > 0$, we have $se^{\frac{\theta x}{k}} - s > 0$. Using the identity $\arctan u + \arctan(1/u) = \pi/2$ for $u > 0$, we obtain

$$S(x;s,k,\theta) = 1 - \frac{2}{\pi} \arctan\left( se^{\frac{\theta x}{k}} - s \right) = \frac{2}{\pi} \cdot \frac{\pi}{2} - \frac{2}{\pi} \arctan\left( se^{\frac{\theta x}{k}} - s \right)$$

$$= \frac{2}{\pi} \left( \frac{\pi}{2} - \arctan\left( se^{\frac{\theta x}{k}} - s \right) \right)$$

$$= \frac{2}{\pi} \arctan\left( \frac{1}{se^{\frac{\theta x}{k}} - s} \right) \tag{3.2}$$

**Proposition 3.1** For all $x > 0$ and $s,k,\theta > 0$,

$$\frac{\partial}{\partial x} S(x;s,k,\theta) = -\frac{2s\theta e^{\frac{\theta x}{k}}}{\pi k (1 + (se^{\frac{\theta x}{k}} - s)^2)} < 0.$$

In particular, $S(\cdot;s,k,\theta)$ is strictly decreasing on $(0,\infty)$ and $0 < S(x;s,k,\theta) < 1$ for all $x > 0$.

*Proof.* Differentiate (3.2) and result follows.

**Proposition 3.2** For $s,k,\theta > 0$,

$$\lim_{x \downarrow 0} S(x;s,k,\theta) = 1, \qquad \lim_{x \uparrow \infty} S(x;s,k,\theta) = 0.$$

*Proof.* Follows directly from proof of Proposition 1.1.

**Lemma 3.2** As $x \downarrow 0$,

$$S(x;s,k,\theta) = 1 - \frac{2s\theta}{\pi k}x + \mathcal{O}(x^2).$$

As $x \uparrow \infty$,

$$S(x;s,k,\theta) = \frac{2}{\pi s}e^{-\frac{\theta x}{k}} + \mathcal{O}(e^{-\frac{3\theta x}{k}}).$$

*Proof.* For $x \downarrow 0$: $e^{\frac{\theta x}{k}} = 1 + \frac{\theta x}{k} + \mathcal{O}(x^2)$, hence $se^{\frac{\theta x}{k}} - s = s\frac{\theta x}{k} + \mathcal{O}(x^2)$ and $\arctan y = y + \mathcal{O}(y^3)$, which gives the linear term. For $x \uparrow \infty$: use Lemma 3.1 with $y = \frac{1}{se^{\frac{\theta x}{k}} - s}$ and $\arctan y = y - \frac{y^3}{3} + \mathcal{O}(y^5)$; since $y \sim \frac{1}{s}e^{-\frac{\theta x}{k}}$, the stated expansion follows.

**Proposition 3.3** Fix $x > 0$. Then, for $s,k,\theta > 0$,

$$\frac{\partial S}{\partial s}(x;s,k,\theta) < 0, \qquad \frac{\partial S}{\partial \theta}(x;s,k,\theta) < 0, \qquad \frac{\partial S}{\partial k}(x;s,k,\theta) > 0.$$

Hence, for fixed $x > 0$, $S$ is strictly decreasing in $s$ and $\theta$, and strictly increasing in $k$.

*Proof.* Differentiate (3.1) with respect to each parameter using $\frac{d}{du}\arctan u = \frac{1}{1+u^2}$ and the chain rule. Since $e^{\frac{\theta x}{k}} > 1$ for $x > 0$, the stated signs follow.

**Lemma 3.3** For every $x > 0$ and $s,k,\theta > 0$,

$$\frac{2}{\pi} \cdot \frac{se^{\frac{\theta x}{k}} - s}{1 + (se^{\frac{\theta x}{k}} - s)^2} \le S(x;s,k,\theta) \le \frac{2}{\pi} \cdot \frac{1}{se^{\frac{\theta x}{k}} - s}.$$

*Proof.* By Lemma 3.1 write $S(x;s,k,\theta) = \frac{2}{\pi}\arctan\left(\frac{1}{se^{\frac{\theta x}{k}} - s}\right)$. For $y \ge 0$ the inequalities $\arctan y \ge \frac{y}{1+y^2}$ and $\arctan y \le y$ yield the stated bounds with $y = \frac{1}{se^{\frac{\theta x}{k}} - s}$.

**Corollary 3.1** There exists $x_0 > 0$ such that, for all $x \ge x_0$,

$$S(x;s,k,\theta) \le \frac{2}{\pi s}e^{-\frac{\theta x}{k}}.$$

*Proof.* From Lemma 3.3, $S(x;s,k,\theta) \le \frac{2}{\pi}\frac{1}{se^{\frac{\theta x}{k}} - s}$. For large $x$, $se^{\frac{\theta x}{k}} - s \ge \frac{1}{2}se^{\frac{\theta x}{k}}$, giving $S(x;s,k,\theta) \le \frac{2}{\pi s}e^{-\frac{\theta x}{k}}$.

### 3.4. Odds

For each $x > 0$ and $s,k,\theta > 0$, we consider the CDF (2.3). The cumulative odds function is defined by

$$O(x;s,k,\theta) := \frac{F(x;s,k,\theta)}{1 - F(x;s,k,\theta)} = \frac{\frac{2}{\pi}\arctan(se^{\frac{\theta x}{k}} - s)}{1 - \frac{2}{\pi}\arctan(se^{\frac{\theta x}{k}} - s)} = \frac{\arctan(se^{\frac{\theta x}{k}} - s)}{\arctan\left(\frac{1}{se^{\frac{\theta x}{k}} - s}\right)} \tag{3.3}$$

**Proposition 4.1** For $s,k,\theta > 0$, $O:(0,\infty) \to (0,\infty)$ is continuous, and

$$\lim_{x \downarrow 0} O(x;s,k,\theta) = 0, \qquad \lim_{x \uparrow \infty} O(x;s,k,\theta) = \infty.$$

*Proof.* Since $0 < F(x;s,k,\theta) < 1$ for $x > 0$, the quotient in (3.3) is well-defined and strictly positive. Continuity follows from continuity of $F$ and $1 - F$. The limits use $F(0^+) = 0$ and $F(\infty) = 1$.

**Proposition 4.2** For all $x > 0$,

$$\frac{d}{dx}O(x;s,k,\theta) = \frac{f(x;s,k,\theta)}{(1 - F(x;s,k,\theta))^2} > 0. \tag{3.4}$$

In particular, $O$ is strictly increasing on $(0,\infty)$.

*Proof.* Differentiate $O = F/(1-F)$; since $F' = f$ and $(1-F)' = -f$,

$$O' = \frac{f(1-F) + Ff}{(1-F)^2} = \frac{f}{(1-F)^2} > 0.$$

**Proposition 4.3** For each fixed $x > 0$,

$$\frac{\partial O}{\partial s}(x;s,k,\theta) > 0, \quad \frac{\partial O}{\partial \theta}(x;s,k,\theta) > 0, \quad \frac{\partial O}{\partial k}(x;s,k,\theta) < 0$$

Hence, for fixed $x > 0$, $O$ is strictly increasing in $s$ and $\theta$, and strictly decreasing in $k$

*Proof.* Differentiate (2.3) with respect to each parameter; apply the chain rule and $\frac{d}{du}\arctan u = \frac{1}{1+u^2}$. Insert these into $\partial O/\partial \cdot = (\partial F/\partial \cdot)/(1-F)^2$.

### 3.5. Log-Odds

The log-odds (logit) is defined by

$$\ell(x;s,k,\theta) := \log\left(\frac{F(x;s,k,\theta)}{1-F(x;s,k,\theta)}\right), \qquad x>0$$

$$= \log F(x;s,k,\theta) - \log(1-F(x;s,k,\theta))$$

$$= \log(\arctan(se^{\frac{\theta x}{k}} - s)) - \log\left(\arctan\left(\frac{1}{se^{\frac{\theta x}{k}} - s}\right)\right) \tag{3.5}$$

**Proposition 5.1** For $s,k,\theta>0$, $\ell:(0,\infty)\to\mathbb{R}$ is continuous and

$$\lim_{x\downarrow 0}\ell(x;s,k,\theta) = -\infty, \qquad \lim_{x\uparrow\infty}\ell(x;s,k,\theta) = +\infty.$$

*Proof.* From corollary 1.1 we have $0<F(x)<1$ for $x>0$, $F(0^+)=0$, and $F(\infty)=1$. Hence $\log F(x)\to-\infty$ and $-\log(1-F(x))\to 0$ as $x\downarrow 0$, while $\log F(x)\to 0$ and $-\log(1-F(x))\to+\infty$ as $x\uparrow\infty$. Continuity follows from continuity of $F$ and $1-F$ on $(0,\infty)$.

**Corollary 5.1** For all $x>0$,

$$F(x;s,k,\theta) = \frac{1}{1+e^{-\ell(x;s,k,\theta)}}, \qquad 1-F(x;s,k,\theta) = \frac{1}{1+e^{\ell(x;s,k,\theta)}}.$$

**Theorem 5.1** For $x>0$,

$$\ell'(x;s,k,\theta) = \frac{f(x;s,k,\theta)}{F(x;s,k,\theta)(1-F(x;s,k,\theta))} > 0. \tag{3.6}$$

In particular, $\ell(\cdot;s,k,\theta)$ is strictly increasing on $(0,\infty)$.

*Proof.* Differentiate (3.5) and use $F'=f$.

**Proposition 5.2** As $x\uparrow\infty$, $\ell'(x;s,k,\theta)\to\theta/k$.

*Proof.* From the survival and density tails, $1-F(x)\sim\frac{2}{\pi s}e^{-\frac{\theta x}{k}}$ and $f(x)\sim\frac{2\theta}{\pi k s}e^{-\frac{\theta x}{k}}$ as $x\uparrow\infty$. Insert these into (3.6).

**Proposition 5.3** For each fixed $x>0$,

$$\frac{\partial\ell}{\partial s}(x;s,k,\theta)>0, \qquad \frac{\partial\ell}{\partial\theta}(x;s,k,\theta)>0, \qquad \frac{\partial\ell}{\partial k}(x;s,k,\theta)<0,$$

Hence, for fixed $x>0$, $\ell$ is strictly increasing in $s$ and $\theta$, and strictly decreasing in $k$

*Proof.* Differentiate (3.5) with respect to each parameter. The signs follow since $e^{\frac{\theta x}{k}}>1$ for $x>0$ and all denominators are positive.

**Remark 5.1** Using the standard bounds $\frac{y}{1+y^2}\le\arctan y\le y$ for $y\ge 0$ in (3.5) yields, for every $x>0$,

$$\log\left(\frac{(se^{\frac{\theta x}{k}}-s)^2}{1+(se^{\frac{\theta x}{k}}-s)^2}\right) \le \ell(x;s,k,\theta) \le \log(1+(se^{\frac{\theta x}{k}}-s)^2). \tag{3.7}$$

These are convenient for tail bracketing and numerical guarding.

### 3.6. Hazard, Cumulative Hazard, and Reversed Hazard

In this section, we study the hazard rate, cumulative and reversed hazard rate functions, which are important indicators in survival analysis.

#### *Hazard Rate Function*

For each $x>0$ and $s,k,\theta>0$, we consider the CDF (2.3), the hazard rate function is given by

$$h(x;s,k,\theta) := \frac{f(x;s,k,\theta)}{S(x;s,k,\theta)} = \frac{\dfrac{2s\theta e^{\frac{\theta x}{k}}}{\pi k(1+(se^{\frac{\theta x}{k}}-s)^2)}}{\dfrac{2}{\pi}\arctan\left(\dfrac{1}{se^{\frac{\theta x}{k}}-s}\right)}$$

$$= \frac{s\theta e^{\frac{\theta x}{k}}}{k(1+(se^{\frac{\theta x}{k}}-s)^2)\arctan\left(\dfrac{1}{se^{\frac{\theta x}{k}}-s}\right)} \tag{3.8}$$

**Proposition 6.1** For every $s,k,\theta>0$, the hazard $h(x;s,k,\theta)$ on $(0,\infty)$ is unimodal with a unique mode $x^*\in(0,\infty)$. Moreover,

$$h(0^+;s,k,\theta) = \frac{2s\theta}{\pi k}, \qquad \lim_{x\to\infty}h(x;s,k,\theta) = \frac{\theta}{k},$$

and the right–tail refinement is

$$h(x;s,k,\theta) = \frac{\theta}{k} + \frac{\theta}{k}e^{-\frac{\theta x}{k}} + O(e^{-2\frac{\theta x}{k}}) \qquad (x\to\infty).$$

*Proof.* Set $u(x) := se^{\frac{\theta x}{k}} - s > 0$ and write

$$h(x;s,k,\theta) = \frac{\theta}{k}\Phi(u(x)), \qquad \Phi(u) := \frac{u+s}{(1+u^2)\arctan(1/u)}, \quad u>0.$$

Since $u'(x)=\frac{\theta}{k}(u+s)>0$, the sign of $h'(x)$ is the sign of $\Phi'(u)$. A direct differentiation yields

$$\Phi'(u)=\frac{N(u)}{(1+u^2)^2\arctan(1/u)^2},$$
$$N(u):=s+u+\arctan(1/u)(1-2su-u^2).$$

The denominator is positive, so $sign(\lambda')=sign(N)$. Now observe that

$$N'(u)=2(u+s)\left(\frac{u}{1+u^2}-\arctan\frac{1}{u}\right)<0 \quad (u>0),$$

because $\arctan t \geq \frac{t}{1+t^2}$ for all $t\geq 0$ applied at $t=1/u$. Hence $N$ is strictly decreasing on $(0,\infty)$. Its endpoint limits are

$$\lim_{u\downarrow 0}N(u)=s+\frac{\pi}{2}>0, \qquad \lim_{u\uparrow\infty}N(u)=-s<0,$$

so by the intermediate value theorem $N$ has a unique zero $u^*>0$. It follows that $\Phi'(u)>0$ for $u<u^*$ and $\Phi'(u)<0$ for $u>u^*$, hence $h$ increases on $\{x:u(x)<u^*\}$ and decreases on $\{x:u(x)>u^*\}$ with a unique mode at the unique $x^*$ solving

$$u(x^*)=se^{\frac{\theta x^*}{k}}-s=u^* \quad \Leftrightarrow \quad x^*=\frac{k}{\theta}\log(1+\frac{u^*}{s}).$$

The endpoint values follow from the small-$x$ and tail expansions already established in Section 3.1.

**Remark 6.1** The unique $u^*$ is characterized by $N(u^*)=0$, i.e.

$$s+u^*+\arctan\left(\frac{1}{u^*}\right)\left(1-2su^*-(u^*)^2\right)=0,$$

and $x^*=\frac{k}{\theta}\log(1+\frac{u^*}{s})$. There is no simpler closed form, but the monotonicity of $N$ makes Newton or bisection immediate.

**Proposition 6.2** For each fixed $x>0$ and $s,k,\theta>0$,

$$\frac{\partial h}{\partial s}(x;s,k,\theta)>0, \qquad \frac{\partial h}{\partial \theta}(x;s,k,\theta)>0, \qquad \frac{\partial h}{\partial k}(x;s,k,\theta)<0.$$

Hence, for fixed $x>0$, $h$ is strictly increasing in $s$ and $\theta$, and strictly decreasing in $k$

*Proof.* Differentiate (3.8) with respect to each parameter and the result follows.

### *Cummulative Hazard Rate Function*

For each $x>0$ and $s,k,\theta>0$, the cummulative hazard rate function (CHRF) is given by

$$H(x;s,k,\theta):=-\log\left(S(x;s,k,\theta)\right)$$
$$=-\log\left(\frac{2}{\pi}\arctan\left(\frac{1}{se^{\frac{\theta x}{k}}-s}\right)\right) \tag{3.9}$$

### *Reversed Hazard Rate Function*

For each $x>0$ and $s,k,\theta>0$, the reversed hazard rate function (RHRF) [29] is given by

$$r(x;s,k,\theta):=\frac{f(x;s,k,\theta)}{F(x;s,k,\theta)}=\frac{\frac{2s\theta e^{\frac{\theta x}{k}}}{\pi k(1+(se^{\frac{\theta x}{k}}-s)^2)}}{\frac{2}{\pi}\arctan(se^{\frac{\theta x}{k}}-s)}$$
$$=\frac{s\theta e^{\frac{\theta x}{k}}}{k(1+(se^{\frac{\theta x}{k}}-s)^2)\arctan(se^{\frac{\theta x}{k}}-s)} \tag{3.10}$$

**Proposition 6.3** For all $x>0$,

$$H'(x;s,k,\theta)=h(x;s,k,\theta), \qquad S(x;s,k,\theta)=e^{-H(x;s,k,\theta)},$$
$$\frac{d}{dx}\log F(x;s,k,\theta)=r(x;s,k,\theta).$$

*Proof.* These follow from $S=1-F$, $F'=f$, and the chain rule.

### 3.7. Moment

Moment of a random variable $X$ is the mean value of the power of the variable. It is essential in defining the distribution of the random since its measures include the mean, variance, etc. For the NGLTGE model, the crude moment is

$$\mu_r^{'}=\frac{2s\theta}{\pi k}\sum_{i=0}^{\infty}\sum_{h=0}^{\infty}\sum_{j=0}^{2i}(-1)^{i+j}\binom{2i}{j}\frac{(2i+1)^h}{h!}\left(\frac{k}{\theta}\right)^{r+1}$$
$$\frac{\Gamma(h+r+1)}{j^{h+r+1}}; \quad r=1,2,\cdots \tag{3.11}$$

Pluggin 1 for r in (3.11) yields the arithmetic mean of $X\sim \text{NGLTGE}(s,k,\theta)$, hence

$$\mu=\frac{2s\theta}{\pi k}\sum_{i=0}^{\infty}\sum_{h=0}^{\infty}\sum_{j=0}^{2i}(-1)^{i+j}\binom{2i}{j}\frac{(2i+1)^h}{h!}\left(\frac{k}{\theta}\right)^{2}\frac{\Gamma(h+2)}{j^{h+2}}.$$

Similarly, one can obtain the 2nd crude moment by replacing r with 2 in (3.11) and so on.

### 3.8. Moment Generating Function

The moment generating function (MGF) of $X\sim NGLTGE(s,k,\theta)$ is

$$M_X(t) = E[e^{tX}] = \int_0^\infty e^{tx} f(x;s,k,\theta)dx, \tag{3.12}$$

whenever the integral is finite.

**Proposition 8.1** For $|t| < \theta / k$ the MGF admits the convergent power series

$$M_X(t) = \sum_{r=0}^{\infty} \frac{\mu_{r'}}{r!} t^r, \qquad \mu_{r'} = \int_0^\infty x^r f(x;s,k,\theta)dx, \tag{3.13}$$

and, substituting the crude moment formula (3.11) for $r \geq 1$ (with $\mu_{0'} = 1$), one obtains

$$M_X(t) = 1 + \frac{2s\theta}{\pi k} \sum_{r=1}^{\infty} \sum_{i=0}^{\infty} \sum_{h=0}^{\infty} \sum_{j=1}^{2i} (-1)^{i+j} \binom{2i}{j} \frac{(2i+1)^h}{h!} \left(\frac{k}{\theta}\right)^{r+1} \frac{\Gamma(h+r+1)}{j^{h+r+1}} \frac{t^r}{r!}. \tag{3.14}$$

The series (3.13)-(3.14) is absolutely and locally uniformly convergent on every compact $|t| \leq t_0 < \theta / k$, hence $M_X$ is analytic on $(-\theta / k, \theta / k)$.

*Proof.* For any fixed $t$ with $|t| < \theta / k$, pick $t_0$ so that $|t| < t_0 < \theta / k$. Using the right-tail behavior of $f$,

$$f(x;s,k,\theta) \sim \frac{2\theta}{\pi k s} e^{-\frac{\theta x}{k}} \quad (x \to \infty),$$

we have for large $x$ the bound $e^{tx} f(x) \leq C e^{-(\frac{\theta}{k} - t_0)x}$, which is integrable on $(0,\infty)$. Hence $e^{tx} f(x)$ is dominated by an integrable function and

$$e^{tx} = \sum_{r=0}^{\infty} \frac{t^r x^r}{r!}$$

can be integrated termwise by dominated convergence (or Tonelli/Fubini on compact $t$-intervals inside $(-\theta / k, \theta / k)$), which yields (3.13). Substituting the crude moment identity (3.11) for $\mu_{r'}$ (valid for $r \geq 1$, with $\mu_{0'} = 1$) gives (3.14). The same domination shows absolute and locally uniform convergence on $|t| \leq t_0 < \theta / k$, proving analyticity there. The restriction $|t| < \theta / k$ is sharp since the tail test applied to (3.12) shows divergence at $t = \theta / k$.

### 3.9. Mean Residual Life Function

For $X \sim NGLTGE(s,k,\theta)$, we consider the survival function (3.2). The mean residual life (MRL) at age $t \geq 0$ is

$$m(t) = E[X - t \mid X > t] = \frac{1}{S(t;s,k,\theta)} \int_t^\infty S(x;s,k,\theta)dx. \tag{3.15}$$

Let $y = e^{\frac{\theta x}{k}}$ so that $x = \frac{k}{\theta} \log y$ and $dx = \frac{k}{\theta} y^{-1} dy$, which maps $x \in (t,\infty)$ to $y \in (e^{\frac{\theta t}{k}}, \infty)$. Then

$$\int_t^\infty S(x)dx = \frac{2k}{\pi\theta} \int_{e^{\frac{\theta t}{k}}}^\infty \frac{\arctan(\frac{1}{s(y-1)})}{y} dy.$$

Now set $u = \frac{1}{s(y-1)}$ (equivalently, $y = 1 + \frac{1}{su}$), so that

$$dy = -\frac{1}{su^2} du, \qquad \frac{dy}{y} = -\frac{1}{u(1+su)} du,$$

and the limits transform as $y = e^{\frac{\theta t}{k}} \mapsto u = \frac{1}{se^{\frac{\theta t}{k}} - s} =: w_t$, while $y \to \infty \mapsto u \downarrow 0$. Therefore

$$\int_t^\infty S(x)dx = \frac{2k}{\pi\theta} \int_0^{w_t} \frac{\arctan(u)}{u(1+su)} du. \tag{3.16}$$

Applying (3.15) yields

$$m(t) = \frac{k}{\theta} \frac{\int_0^{w_t} \frac{\arctan(u)}{u(1+su)} du}{\arctan(w_t)}, \qquad w_t := \frac{1}{se^{\frac{\theta t}{k}} - s}. \tag{3.17}$$

Alternatively, from (3.16), integrate by parts with

$$u_1 = \arctan(u), \qquad dv_1 = \frac{du}{u(1+su)} = (\frac{1}{u} - \frac{s}{1+su})du,$$

so that

$$du_1 = \frac{du}{1+u^2}, \qquad v_1 = \log(\frac{u}{1+su}).$$

Hence,

$$\int_0^{w_t} \frac{\arctan(u)}{u(1+su)} du = [\arctan(u)\log(\tfrac{u}{1+su})]_0^{w_t} - \int_0^{w_t} \frac{\log(\frac{u}{1+su})}{1+u^2} du.$$

The boundary term at $u = 0$ vanishes, and at $u = w_t$ we have

$$\log(\frac{w_t}{1+sw_t}) = \log(\frac{1}{se^{\frac{\theta t}{k}}}) = -\log s - \frac{\theta}{k} t.$$

Therefore, (3.16) implies

$$\int_t^{\infty} S(x)dx = \frac{2k}{\pi\theta}\left[\arctan(w_t)(-\log s - \frac{\theta}{k}t) - \int_0^{w_t} \frac{\log(\frac{u}{1+su})}{1+u^2}du\right],$$

and dividing by $S(t) = \frac{2}{\pi}\arctan(w_t)$ gives

$$m(t) = \frac{k}{\theta}\left[-\log(se^{\frac{\theta t}{k}}) - \frac{1}{\arctan(w_t)}\int_0^{w_t} \frac{\log(\frac{u}{1+su})}{1+u^2}du\right], \quad w_t = \frac{1}{se^{\frac{\theta t}{k}} - s}. \tag{3.18}$$

which is an alternative representation of (3.17).

### 3.10. Stochastic Orderings

The following corollary follows from Proposition (2.2).

**Corollary 10.1 (Usual stochastic order)** Fix any two parameter triples that differ in only one coordinate.

1. If $s_2 > s_1$ (with $k,\theta$ fixed), then $F(\cdot;s_2,k,\theta) \geq F(\cdot;s_1,k,\theta)$ and hence

$$X(s_2,k,\theta) \leq_{st} X(s_1,k,\theta).$$

2. If $\theta_2 > \theta_1$ (with $s,k$ fixed), then

$$X(s,k,\theta_2) \leq_{st} X(s,k,\theta_1).$$

3. If $k_2 > k_1$ (with $s,\theta$ fixed), then

$$X(s,k_1,\theta) \leq_{st} X(s,k_2,\theta).$$

The following corollary follows from Proposition (6.2).

**Corollary 10.2 (Hazard--rate order)** Fix two parameter triples that differ in only one coordinate.

1. If $s_2 > s_1$ (with $k,\theta$ fixed), then $h(x;s_2,k,\theta) \geq h(x;s_1,k,\theta)\ \forall x > 0,$ hence

$$X(s_2,k,\theta) \leq_{hr} X(s_1,k,\theta).$$

2. If $\theta_2 > \theta_1$ (with $s,k$ fixed), then

$$X(s,k,\theta_2) \leq_{hr} X(s,k,\theta_1).$$

3. If $k_2 > k_1$ (with $s,\theta$ fixed), then

$$X(s,k_1,\theta) \leq_{hr} X(s,k_2,\theta).$$

**Corollary 10.3** In each case above, $X \leq_{hr} Y \Rightarrow X \leq_{st} Y$.

**Remark 10.1** For two parameter sets

$$\eta_1 = (s_1,k_1,\theta_1), \qquad \eta_2 = (s_2,k_2,\theta_2),$$

the ratio $f(\cdot;\eta_2)/f(\cdot;\eta_1)$ is not monotone in $x$ in general, so a global likelihood–ratio order across $s$, $k$, or $\theta$ does not hold without further restrictions.

### 3.11. Order Statistics

Let $X_1,\ldots,X_n$ be an i.i.d. sample from $NGLTGE(s,k,\theta)$ with CDF (2.3) and PDF (2.4). We denote the *order index* by $r \in \{1,\ldots,n\}$. The CDF and PDF of $X_{r:n}$ are

$$F_{r:n}(x) = \sum_{j=r}^{n}\binom{n}{j}[F(x)]^j[1-F(x)]^{n-j},$$

$$f_{r:n}(x) = \frac{n!}{(r-1)!(n-r)!}[F(x)]^{r-1}[1-F(x)]^{n-r}f(x), \quad x > 0,$$

Using the definitions (2.3) and (2.4), we obtain

$$f_{r:n}(x) = \frac{n!}{(r-1)!(n-r)!}\left[\frac{2}{\pi}\arctan(se^{\frac{\theta x}{k}} - s)\right]^{r-1}$$

$$\left[\frac{2}{\pi}\arctan\left(\frac{1}{se^{\frac{\theta x}{k}} - s}\right)\right]^{n-r}$$

$$\times \frac{2s\theta e^{\frac{\theta x}{k}}}{\pi k(1+(se^{\frac{\theta x}{k}} - s)^2)}, \qquad x > 0.$$

Moreover, the CDF and PDF of the minimum $X_{1:n}$ are given by

$$F_{1:n}(x) = 1-[1-F(x)]^n = 1-\left[\frac{2}{\pi}\arctan(\frac{1}{se^{\frac{\theta x}{k}} - s})\right]^n,$$

$$f_{1:n}(x) = n[1-F(x)]^{n-1}f(x) = n\left[\frac{2}{\pi}\arctan(\frac{1}{se^{\frac{\theta x}{k}} - s})\right]^{n-1}$$

$$\frac{2s\theta e^{\frac{\theta x}{k}}}{\pi k(1+(se^{\frac{\theta x}{k}} - s)^2)}.$$

Finally, the CDF and PDF of the maximum $X_{n:n}$ are given by

$$F_{n:n}(x) = [F(x)]^n = \left[\frac{2}{\pi}\arctan(se^{\frac{\theta x}{k}} - s)\right]^n,$$

$$f_{n:n}(x) = n[F(x)]^{n-1} f(x) = n\left[\frac{2}{\pi}\arctan(se^{\frac{\theta x}{k}} - s)\right]^{n-1} \frac{2s\theta e^{\frac{\theta x}{k}}}{\pi k(1+(se^{\frac{\theta x}{k}} - s)^2)}.$$

### 3.12. Rényi Entropy

Let $X \sim NGLTGE(s,k,\theta)$ with density (2.4). For $\alpha > 0$, $\alpha \neq 1$, the Rényi entropy is

$$H_\alpha(X) = \frac{1}{1-\alpha}\log\left(\int_0^\infty f(x;s,k,\theta)^\alpha dx\right).$$

With the substitutions $y = e^{\frac{\theta x}{k}}$ (so $dx = \frac{k}{\theta}y^{-1}dy$, $y \in (1,\infty)$) and then $u = s(y-1)$, one obtains

$$\int_0^\infty f(x)^\alpha dx = \left(\frac{2s\theta}{\pi k}\right)^\alpha \int_1^\infty \frac{y^\alpha}{(1+s^2(y-1)^2)^\alpha}\frac{k}{\theta}\frac{dy}{y} =$$

$$\frac{2^\alpha}{\pi^\alpha}s^{\alpha-1}\theta^{\alpha-1}k^{1-\alpha}\int_0^\infty \frac{(1+\frac{u}{s})^{\alpha-1}}{(1+u^2)^\alpha}du$$

Hence

$$H_\alpha(X) = \frac{1}{1-\alpha}\begin{bmatrix}(\alpha-1)\log(\frac{s\theta}{k}) + \alpha\log 2 \\ -\alpha\log\pi + \log(\mathcal{J}_\alpha(s))\end{bmatrix},$$

with

$$\mathcal{J}_\alpha(s) = \int_0^\infty \frac{(1+\frac{u}{s})^{\alpha-1}}{(1+u^2)^\alpha}du$$

**Remark 12.1** For every $\alpha > 0$, the integral $\int_0^\infty f(x)^\alpha dx$ is finite: near $u = 0$ the integrand is bounded; as $u \to \infty$ it behaves like $u^{-(\alpha+1)}$, which is integrable. Thus $H_\alpha(X)$ exists for all $\alpha > 0$, $\alpha \neq 1$.

Collision entropy ($\alpha = 2$).

For $\alpha = 2$,

$$\mathcal{J}_2(s) = \int_0^\infty \frac{1+\frac{u}{s}}{(1+u^2)^2}du = \frac{\pi}{4} + \frac{1}{2s},$$

so

$$\int_0^\infty f(x)^2 dx = \frac{\theta}{k}\left(\frac{s}{\pi} + \frac{2}{\pi^2}\right), \qquad H_2(X) = -\log\left[\frac{\theta}{k}\left(\frac{s}{\pi} + \frac{2}{\pi^2}\right)\right].$$

Asymptotics in $s$.

As $s \to \infty$,

$$\mathcal{J}_\alpha(s) \to \int_0^\infty \frac{du}{(1+u^2)^\alpha} = \frac{\sqrt{\pi}\,\Gamma(\alpha-\frac{1}{2})}{2\Gamma(\alpha)},$$

so

$$H_\alpha(X) = -\log s + \frac{1}{1-\alpha}\begin{bmatrix}\alpha\log 2 - \alpha\log\pi + \\ \log\frac{\sqrt{\pi}\,\Gamma(\alpha-\frac{1}{2})}{2\Gamma(\alpha)} + (\alpha-1)\log(\frac{\theta}{k})\end{bmatrix} + o(1).$$

As $s \downarrow 0$,

$$\mathcal{J}_\alpha(s) \sim s^{1-\alpha}\int_0^\infty \frac{u^{\alpha-1}}{(1+u^2)^\alpha}du = \frac{1}{2}s^{1-\alpha}B\left(\frac{\alpha}{2},\frac{\alpha}{2}\right),$$

and the exterior factor $s^{\alpha-1}$ cancels, so $\int f^\alpha$ converges to a finite positive limit and $H_\alpha(X)$ tends to a constant.

### 3.13. Stress–Strength Reliability

Let $X \sim NGLTGE(s_1,k_1,\theta_1)$ denote the *strength* and $Y \sim NGLTGE(s_2,k_2,\theta_2)$ the *stress*, independent. With CDF (2.3) and PDF (2.4), the stress–strength reliability [30-34] is

$$R = \Pr(X > Y) = \int_0^\infty S_Y(x) f_X(x)dx = \int_0^\infty (1-F_Y(x)) f_X(x)dx. \quad (3.19)$$

Starting from (3.19),

$$R = \int_0^\infty (1-F_Y(x)) f_X(x)dx.$$

Using the CDF in (2.3) for $Y$,

$$1 - F_Y(x) = 1 - \frac{2}{\pi}\arctan(s_2 e^{\frac{\theta_2 x}{k_2}} - s_2) = \frac{2}{\pi}\arctan\left(\frac{1}{s_2 e^{\frac{\theta_2 x}{k_2}} - s_2}\right),$$

Next, perform the change of variables

$$y = e^{\frac{\theta_1 x}{k_1}} \quad \Rightarrow \quad dx = \frac{k_1}{\theta_1}\frac{dy}{y}, \qquad y \in (1,\infty).$$

By the PDF in (2.4) for $X$,

$$f_X(x)dx = \frac{2s_1\theta_1 e^{\frac{\theta_1 x}{k_1}}}{\pi k_1\left(1+(s_1 e^{\frac{\theta_1 x}{k_1}}-s_1)^2\right)}\cdot\frac{k_1}{\theta_1}\frac{dy}{y} = \frac{2s_1}{\pi}\frac{dy}{1+(s_1y-s_1)^2}.$$

For the same $x$, we have

$$e^{\frac{\theta_2 x}{k_2}} = (e^{\frac{\theta_1 x}{k_1}})^{\frac{\theta_2 k_1}{\theta_1 k_2}} = y^a, \qquad a := \frac{\theta_2 k_1}{\theta_1 k_2} > 0.$$

Therefore

$$1 - F_Y(x) = \frac{2}{\pi}\arctan\left(\frac{1}{s_2 y^a - s_2}\right),$$

and substituting into (3.19) yields the single-integral closed form

$$R = \frac{4s_1}{\pi^2}\int_1^\infty \frac{\arctan\left(\frac{1}{s_2 y^a - s_2}\right)}{1+(s_1y-s_1)^2}dy, \qquad a = \frac{\theta_2 k_1}{\theta_1 k_2}.$$

A numerically convenient equivalent form follows under $u = s_1(y-1)$ (so $y = 1+\frac{u}{s_1}$, $dy = \frac{du}{s_1}$, $u \in (0,\infty)$):

$$R = \frac{4}{\pi^2}\int_0^\infty \frac{\arctan\left(\frac{1}{s_2((1+\frac{u}{s_1})^a - 1)}\right)}{1+u^2}du,$$

which has a $(1+u^2)^{-1}$ kernel that damps the tail.

In Figure **2**, the trend of panel 4 indicates the mean of the distribution to be a monotonic surface that decreases with increases in the parameters and thus to signify a uniform trend. Variance, as shown in panel 5,

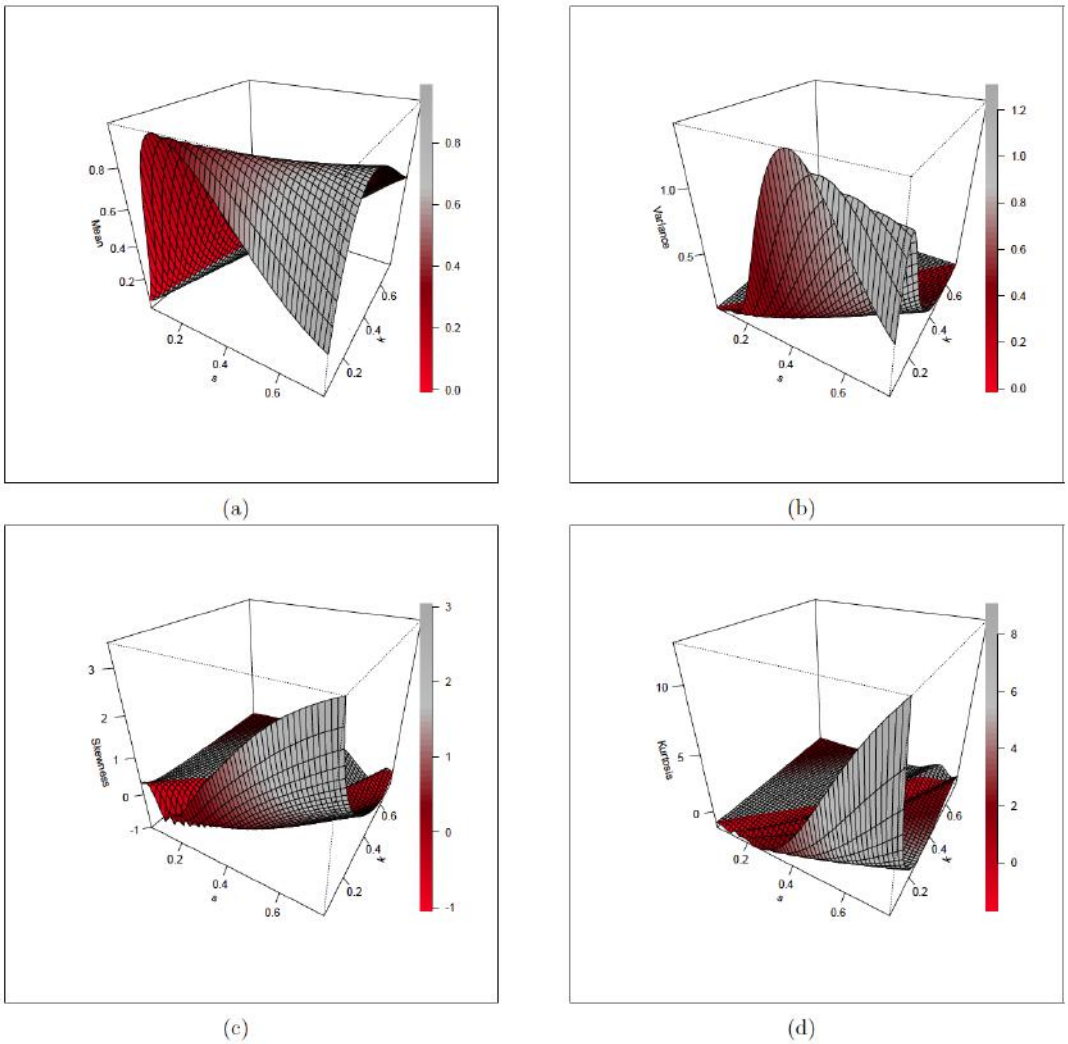


**Figure 2:** Plots of (**a**) Mean, (**b**) Variance, (**c**) Skewness and (**d**) Kurtosis of NGLTGE distribution.

has an evident peak that signifies that there is one set of parameters to which the spread or variability of the distribution is optimized. This exercise is fascinating in that it picks out a region of high variability in the parameter space. The skewness plot for panel 6 is one of flat surface with variation, which means that the asymmetry of the distribution does not shift markedly across the parameter space but is fairly stable. Finally, the kurtosis plot for panel 7 is similar to that of the variance with a clear peak. This peak shows that the tail heaviness of the distribution is highest for a particular set of parameter values, implying a greater chance of outlier values than for a normal distribution for that particular point.

## 4. PARAMETER ESTIMATION

In this section, the parameters of the NGLTGE model namely $s,k$ and $\theta$ are estimated using some non-Bayesian estimation procedures; viz, Maximum likelihood, Maximum product of spacing, Least squares, Weighted least squares and Cramér-von Mises methods.

### 4.1. Maximum Likelihood Estimation (MLE)

Consider a random sample of size $n$, denoted by $x_1,x_2,\ldots,x_n$, where each observation is independently and identically distributed (i.i.d.) following the New Generalized Lomax Tangent Transformed Exponential (NGLTGE) distribution with parameters $s$, $k$ and $\theta$.

The PDF of the NGLTGE distribution, substituting the Exponential baseline $g(x;\theta)=\theta e^{-\theta x}$ and $G(x;\theta)=1-e^{-\theta x}$ into Equation (3), is correctly formulated as:

$$f(x;s,k,\theta)=\left(\frac{2s\theta}{\pi k}\right)\frac{e^{\frac{\theta x}{k}}}{1+\left(se^{\frac{\theta x}{k}}-s\right)^2}$$

The likelihood function, $\mathcal{L}(s,k,\theta\,|\,\mathbf{x})$, is the product of the densities:

$$\mathcal{L}(s,k,\theta\,|\,\mathbf{x})=\prod_{i=1}^{n}f(x_i;s,k,\theta)$$

Consequently, the correct log-likelihood function, $\ell(s,k,\theta)=\log\left[\mathcal{L}\right]$, is derived as:

$$\ell(s,k,\theta)=n\log\left(\frac{2\theta}{\pi}\right)+n\log(s)-n\log(k)+\frac{\theta}{k}\sum_{i=1}^{n}x_i$$
$$-\sum_{i=1}^{n}\log\left[1+\left(se^{\frac{\theta x_i}{k}}-s\right)^2\right]$$

The Maximum Likelihood Estimators (MLEs) of the parameters $\hat{\Theta}=(\hat{s},\hat{k},\hat{\theta})$ are obtained by simultaneously solving the system of score equations, $\nabla\ell=\mathbf{0}$, where $\nabla\ell=(\frac{\partial\ell}{\partial s},\frac{\partial\ell}{\partial k},\frac{\partial\ell}{\partial\theta})^T$.

Let $W_i=s\left(e^{\frac{\theta x_i}{k}}-1\right)$, such that $W_i+s=se^{\frac{\theta x_i}{k}}$.

#### *4.1.1. Score Equations*

The partial derivatives (score equations) are:

$$\frac{\partial\ell}{\partial s}=\frac{n}{s}-\sum_{i=1}^{n}\frac{2W_i}{1+W_i^2}\cdot\left(e^{\frac{\theta x_i}{k}}-1\right)=0, \tag{4.1}$$

$$\frac{\partial\ell}{\partial k}=-\frac{n}{k}-\frac{\theta}{k^2}\sum_{i=1}^{n}x_i-\sum_{i=1}^{n}\frac{2W_i}{1+W_i^2}\cdot\left(-\frac{s\theta x_i}{k^2}e^{\frac{\theta x_i}{k}}\right)=0, \tag{4.2}$$

and

$$\frac{\partial\ell}{\partial\theta}=\frac{n}{\theta}+\frac{1}{k}\sum_{i=1}^{n}x_i-\sum_{i=1}^{n}\frac{2W_i}{1+W_i^2}\cdot\left(\frac{sx_i}{k}e^{\frac{\theta x_i}{k}}\right)=0. \tag{4.3}$$

### 4.2. Numerical Optimization Component

The system of coupled, non-linear score equations (Eqs. (4.1)-(4.3)) cannot be solved analytically for the MLEs. Therefore, a numerical maximization technique is required to find the parameter estimates that maximize the log-likelihood function $\ell(s,k,\theta)$.

#### *4.2.1. Optimization Algorithm*

The MLEs are typically obtained using iterative, gradient-based optimization algorithms. The most common choice is a Quasi-Newton method such as the Broyden-Fletcher-Goldfarb-Shanno (BFGS) algorithm. BFGS iteratively updates the parameter vector $\Theta$ by utilizing the gradient (score equations) and approximating the inverse of the Hessian matrix (matrix of second partial derivatives), thus avoiding the complex derivation of the analytical second derivatives.

#### *4.2.2. Initial Values and Constraints*

1. **Initial Guess ($\Theta_0$):** The choice of starting values $(s_0,k_0,\theta_0)$ is critical for the convergence and efficiency of the optimizer. A common practice is to use simple moment estimators for the baseline distribution (e.g., $\hat{\theta}_0=1/\bar{x}$) and set $s_0=1$ and $k_0=1$, or use estimators obtained via the Method of Least Squares (LSE) or Cramer-von Mises (CVM) methods for a more robust start.

2. **Constraints:** The optimization must be performed under the parameter space constraints: $s>0$, $k>0$, and $\theta>0$. The numerical solver must be configured to respect these boundaries (constrained optimization).

#### 4.2.3. Asymptotic Properties

The Monte Carlo simulation confirms the good asymptotic behavior of the estimators. This is theoretically underpinned by the standard properties of MLE, which state that as the sample size $n\to\infty$, the MLE vector $\hat{\Theta}$ is consistent, asymptotically normally distributed, and asymptotically efficient. The asymptotic variance-covariance matrix of the MLEs is estimated by the inverse of the observed Fisher information matrix, often calculated as the negative inverse of the Hessian matrix evaluated at $\hat{\Theta}$.

$$V(\hat{\Theta})\approx -H^{-1}(\hat{\Theta})$$

### 4.3. Maximum Product of Spacing (MPS) Estimation

The MPS method, proposed by [35], is a stable alternative to MLE, particularly useful for distributions with heavy tails or when the likelihood function is poorly behaved. The technique focuses on maximizing the geometric mean of the differences (spacings) between consecutive values of the NGLTGE Cumulative Distribution Function (CDF), $F(x)$, evaluated at the ordered data points $x_{j:n}$. The MPS estimators ($\hat{s}_{MPS},\hat{k}_{MPS},\hat{\theta}_{MPS}$) are obtained by maximizing the log-product of spacings, $N(\Theta)$:

$$N(s,k,\theta)=\frac{1}{n+1}\sum_{j=1}^{n+1}\ln\left[F\left(x_{j:n}\mid\Theta\right)-F\left(x_{j-1:n}\mid\Theta\right)\right], \tag{4.4}$$

where $F\left(x_{0:n}\right)=0$ and $F\left(x_{n+1:n}\right)=1$.

### 4.4. Least Squares Estimation (LSE)

The LSE method, first proposed by [36], belongs to the family of minimum distance estimators. The LSE principle minimizes the sum of squared differences between the theoretical CDF, $F\left(x_{j:n}\mid\Theta\right)$, and the empirical plotting position, $\frac{j}{n+1}$, for the ordered observations. The LSE estimators ($\hat{s}_{LSE},\hat{k}_{LSE},\hat{\theta}_{LSE}$) are computed by minimizing the objective function $L(\Theta)$:

$$L(s,k,\theta)=\arg\min_{\Theta}\sum_{j=1}^{n}\left[F\left(x_{j:n}\mid\Theta\right)-\frac{j}{n+1}\right]^2. \tag{4.5}$$

### 4.5. Weighted Least Squares Estimation (WLSE)

WLSE is a refined version of LSE that accounts for the varying precision of the ordered statistics. The method minimizes a weighted sum of squared differences, using weights ($w_j$) inversely proportional to the variance of the plotting positions. This naturally gives less influence to the extreme observations and improves the stability of the estimates. The weights are given by $w_j=\frac{(n+1)^2(n+2)}{j(n-j+1)}$. The WLSE estimators ($\hat{s}_{WLSE},\hat{k}_{WLSE},\hat{\theta}_{WLSE}$) minimize the objective function $W(\Theta)$:

$$W(s,k,\theta)=\arg\min_{\Theta}\sum_{j=1}^{n}w_j\left[F\left(x_{j:n}\mid\Theta\right)-\frac{j}{n+1}\right]^2. \tag{4.6}$$

### 4.6. Cramer-von Mises Estimation (CvM)

The CvM method is another robust minimum distance estimator that aims to minimize the quadratic distance between the empirical and theoretical CDFs across the entire distribution. This method is known for providing a good overall fit and stability. The CvM estimators ($\hat{s}_{CvM},\hat{k}_{CvM},\hat{\theta}_{CvM}$) are derived by minimizing the CvM criterion function $W_{CvM}(\Theta)$:

$$W_{CvM}\left(s,k,\theta\right)=\arg\min_{\Theta}\left\{\frac{1}{12n}+\sum_{j=1}^{n}\left[F\left(x_{j:n}\mid\Theta\right)-\frac{2j-1}{2n}\right]^2\right\}.$$

The non-linear systems of equations resulting from these minimization criteria require the use of numerical optimization techniques.

## 5. MONTE CARLO SIMULATION STUDY

For the parameters $\xi=(s,k,\theta)$ of the NGLTGE distribution, a Monte Carlo simulation of 10,000 replicates was demonstrated at sample sizes $n=15,25,75$ and $100$ with true parameter settings (a) $s=0.05,k=0.75,\theta=0.2$ (b) $s=0.07,k=0.80,\theta=0.35$ (c) $s=0.05,k=0.70,\theta=0.45$ (d) $s=0.08,k=0.55,\theta=0.7$. The average bias and Root Mean Squared Error (RMSE) were computed, where

$$bias(\xi)=\frac{1}{N}\sum_{i=1}^{N}\left(\hat{\xi}_i-\xi_0\right);\quad and\quad RMSE(\xi)=\sqrt{\frac{1}{N}\sum_{i=1}^{N}\left(\hat{\xi}_i-\xi_0\right)^2}.$$

Tables **1** and **2** contain the results of the simulation.

The simulation results in Tables **1** and **2** display how the performances of different estimators; MLE, MPS, LS, WLS, and CvM change for different sample

**Table 1: Simulation Results for True Value Settings (a) and (b)**

| True Value | Estimator | Parameter | $n=15$ | | $n=25$ | | $n=75$ | | $n=100$ | |
|---|---|---|---|---|---|---|---|---|---|---|
| | | | **bias** | **RMSE** | **bias** | **RMSE** | **bias** | **RMSE** | **bias** | **RMSE** |
| $s=0.05,$ $k=0.75,$ $\theta=0.2$ | MLE | $\hat{s}$ | 0.01243 | 0.07021 | 0.00796 | 0.04811 | 0.00232 | 0.02355 | 0.00158 | 0.01989 |
| | | $\hat{k}$ | 0.01737 | 0.13329 | 0.01596 | 0.09636 | 0.01253 | 0.05760 | 0.00817 | 0.05064 |
| | | $\hat{\theta}$ | 0.01716 | 0.05022 | 0.01056 | 0.03875 | 0.00601 | 0.02237 | 0.00414 | 0.01775 |
| | MPS | $\hat{s}$ | 0.06462 | 0.13905 | 0.03775 | 0.07860 | 0.01304 | 0.02949 | 0.00995 | 0.02352 |
| | | $\hat{k}$ | 0.11265 | 0.26302 | 0.06964 | 0.15738 | 0.03125 | 0.07560 | 0.02355 | 0.06324 |
| | | $\hat{\theta}$ | 0.00527 | 0.04096 | 0.00576 | 0.03134 | 0.00223 | 0.01773 | 0.00252 | 0.01338 |
| | LS | $\hat{s}$ | 0.05619 | 0.16969 | 0.02951 | 0.07665 | 0.00807 | 0.02910 | 0.00610 | 0.02434 |
| | | $\hat{k}$ | 0.05517 | 0.15708 | 0.03623 | 0.11089 | 0.02145 | 0.06623 | 0.01547 | 0.05809 |
| | | $\hat{\theta}$ | 0.00405 | 0.05251 | 0.00191 | 0.04291 | 0.00280 | 0.02672 | 0.00162 | 0.02144 |
| | WLS | $\hat{s}$ | 0.04684 | 0.13363 | 0.02387 | 0.06890 | 0.00567 | 0.02619 | 0.00399 | 0.02168 |
| | | $\hat{k}$ | 0.08409 | 0.25586 | 0.04171 | 0.14502 | 0.01741 | 0.07263 | 0.01283 | 0.06182 |
| | | $\hat{\theta}$ | 0.00311 | 0.04493 | 0.00163 | 0.03689 | 0.00338 | 0.02244 | 0.00264 | 0.01899 |
| | CvM | $\hat{s}$ | 0.02158 | 0.10135 | 0.01291 | 0.05863 | 0.00354 | 0.02630 | 0.00277 | 0.02253 |
| | | $\hat{k}$ | 0.01580 | 0.11615 | 0.01275 | 0.08442 | 0.01269 | 0.06102 | 0.01161 | 0.06421 |
| | | $\hat{\theta}$ | 0.01212 | 0.05154 | 0.00781 | 0.04253 | 0.00571 | 0.02666 | 0.00464 | 0.02477 |
| $s=0.07,$ $k=0.80,$ $\theta=0.35$ | MLE | $\hat{s}$ | 0.00845 | 0.07775 | 0.00852 | 0.06253 | 0.00190 | 0.03012 | 0.00093 | 0.02592 |
| | | $\hat{k}$ | 0.01288 | 0.14034 | 0.01745 | 0.11718 | 0.01035 | 0.06325 | 0.00855 | 0.05641 |
| | | $\hat{\theta}$ | 0.03231 | 0.08539 | 0.02068 | 0.06372 | 0.00905 | 0.03370 | 0.00779 | 0.02833 |
| | MPS | $\hat{s}$ | 0.07238 | 0.15591 | 0.04710 | 0.10113 | 0.01500 | 0.03807 | 0.01088 | 0.03106 |
| | | $\hat{k}$ | 0.12534 | 0.27409 | 0.08517 | 0.19264 | 0.03411 | 0.08287 | 0.02711 | 0.07106 |
| | | $\hat{\theta}$ | 0.00656 | 0.06476 | 0.00601 | 0.05216 | 0.00194 | 0.02850 | 0.00064 | 0.02464 |
| | LS | $\hat{s}$ | 0.06031 | 0.15742 | 0.03817 | 0.10758 | 0.00963 | 0.03694 | 0.00767 | 0.03211 |
| | | $\hat{k}$ | 0.05605 | 0.16002 | 0.04036 | 0.11998 | 0.02164 | 0.07765 | 0.01589 | 0.05883 |
| | | $\hat{\theta}$ | 0.00584 | 0.08229 | 0.00392 | 0.06438 | 0.00356 | 0.04637 | 0.00169 | 0.03337 |
| | WLS | $\hat{s}$ | 0.04996 | 0.14011 | 0.02913 | 0.08796 | 0.00673 | 0.03369 | 0.00445 | 0.02868 |
| | | $\hat{k}$ | 0.09001 | 0.27213 | 0.05097 | 0.17690 | 0.01698 | 0.08072 | 0.01535 | 0.07095 |
| | | $\hat{\theta}$ | 0.00814 | 0.07807 | 0.00410 | 0.05206 | 0.00403 | 0.03266 | 0.00537 | 0.03534 |
| | CvM | $\hat{s}$ | 0.01856 | 0.10072 | 0.01580 | 0.08216 | 0.00358 | 0.03350 | 0.00322 | 0.02980 |
| | | $\hat{k}$ | 0.00513 | 0.11891 | 0.01502 | 0.10846 | 0.01006 | 0.06482 | 0.00864 | 0.05667 |
| | | $\hat{\theta}$ | 0.02207 | 0.08504 | 0.01558 | 0.07441 | 0.00807 | 0.04024 | 0.00586 | 0.03568 |

**Table 2: Simulation Results for True Value Settings (c) and (d)**

| True Value | Estimator | Parameter | $n=15$ | | $n=25$ | | $n=75$ | | $n=100$ | |
|---|---|---|---|---|---|---|---|---|---|---|
| | | | **bias** | **RMSE** | **bias** | **RMSE** | **bias** | **RMSE** | **bias** | **RMSE** |
| $s=0.05,$ $k=0.70,$ $\theta=0.45$ | MLE | $\hat{s}$ | 0.00954 | 0.06759 | 0.00683 | 0.04747 | 0.00148 | 0.02298 | 0.00147 | 0.02005 |
| | | $\hat{k}$ | 0.00495 | 0.13435 | 0.00741 | 0.10421 | 0.00755 | 0.06274 | 0.00584 | 0.04983 |
| | | $\hat{\theta}$ | 0.03331 | 0.09179 | 0.02232 | 0.06818 | 0.01081 | 0.04223 | 0.00843 | 0.03272 |
| | MPS | $\hat{s}$ | 0.06009 | 0.13350 | 0.03577 | 0.07661 | 0.01131 | 0.02896 | 0.00911 | 0.02424 |
| | | $\hat{k}$ | 0.10829 | 0.23957 | 0.06965 | 0.16231 | 0.02923 | 0.07573 | 0.02336 | 0.06129 |
| | | $\hat{\theta}$ | 0.00746 | 0.07504 | 0.00619 | 0.05446 | 0.00178 | 0.03121 | 0.00097 | 0.02744 |
| | LS | $\hat{s}$ | 0.04928 | 0.14618 | 0.02799 | 0.07446 | 0.00690 | 0.02848 | 0.00541 | 0.02386 |
| | | $\hat{k}$ | 0.05458 | 0.16479 | 0.03889 | 0.11690 | 0.01858 | 0.07143 | 0.01630 | 0.06486 |
| | | $\hat{\theta}$ | 0.00638 | 0.08640 | 0.00032 | 0.07279 | 0.00543 | 0.04677 | 0.00642 | 0.04815 |
| | WLS | $\hat{s}$ | 0.04115 | 0.12009 | 0.02181 | 0.06545 | 0.00460 | 0.02550 | 0.00376 | 0.02193 |
| | | $\hat{k}$ | 0.07240 | 0.22797 | 0.03972 | 0.15316 | 0.01441 | 0.07654 | 0.01079 | 0.06260 |
| | | $\hat{\theta}$ | 0.00619 | 0.07596 | 0.00717 | 0.06644 | 0.00679 | 0.04254 | 0.00579 | 0.03655 |
| | CvM | $\hat{s}$ | 0.01722 | 0.09149 | 0.01183 | 0.05726 | 0.00246 | 0.02587 | 0.00212 | 0.02215 |
| | | $\hat{k}$ | 0.00360 | 0.12074 | 0.00753 | 0.09730 | 0.01013 | 0.06955 | 0.00913 | 0.05973 |
| | | $\hat{\theta}$ | 0.02129 | 0.08567 | 0.01509 | 0.07090 | 0.01176 | 0.04754 | 0.01058 | 0.04448 |
| $s=0.08,$ $k=0.50,$ $\theta=0.70$ | MLE | $\hat{s}$ | 0.01669 | 0.11103 | 0.00603 | 0.06645 | 0.00181 | 0.03390 | 0.00038 | 0.02857 |
| | | $\hat{k}$ | 0.00653 | 0.13791 | 0.00466 | 0.10138 | 0.00288 | 0.05403 | 0.00239 | 0.04601 |
| | | $\hat{\theta}$ | 0.02987 | 0.08751 | 0.02680 | 0.07624 | 0.01087 | 0.03867 | 0.01351 | 0.04043 |
| | MPS | $\hat{s}$ | 0.09631 | 0.23061 | 0.04821 | 0.10755 | 0.01629 | 0.04259 | 0.01153 | 0.03414 |
| | | $\hat{k}$ | 0.12152 | 0.25084 | 0.07284 | 0.15762 | 0.02748 | 0.06818 | 0.02064 | 0.05599 |
| | | $\hat{\theta}$ | 0.00204 | 0.05653 | 0.00322 | 0.04697 | 0.00205 | 0.02928 | 0.00498 | 0.03006 |
| | LS | $\hat{s}$ | 0.08720 | 0.27201 | 0.03804 | 0.10783 | 0.01089 | 0.04270 | 0.00654 | 0.03349 |
| | | $\hat{k}$ | 0.09199 | 0.28570 | 0.04241 | 0.13396 | 0.01554 | 0.06407 | 0.00992 | 0.05349 |
| | | $\hat{\theta}$ | 0.00434 | 0.06213 | 0.00021 | 0.05076 | 0.00360 | 0.03232 | 0.00616 | 0.03500 |
| | WLS | $\hat{s}$ | 0.07250 | 0.22604 | 0.02811 | 0.09259 | 0.00713 | 0.03792 | 0.00405 | 0.03114 |
| | | $\hat{k}$ | 0.09042 | 0.27937 | 0.03878 | 0.13990 | 0.01126 | 0.06114 | 0.00760 | 0.05277 |
| | | $\hat{\theta}$ | 0.00934 | 0.05388 | 0.01261 | 0.06844 | 0.00647 | 0.03095 | 0.00970 | 0.03838 |
| | CvM | $\hat{s}$ | 0.03145 | 0.15990 | 0.01391 | 0.08269 | 0.00407 | 0.03879 | 0.00160 | 0.03124 |
| | | $\hat{k}$ | 0.01604 | 0.18152 | 0.00592 | 0.10988 | 0.00376 | 0.06001 | 0.00201 | 0.05175 |
| | | $\hat{\theta}$ | 0.01493 | 0.06509 | 0.01320 | 0.06028 | 0.00727 | 0.03370 | 0.01005 | 0.03959 |

sizes ($n$) for four different true parameter values ($s,k,\theta$). Performance is considered on the basis of bias and RMSE. The smaller the values of bias and RMSE, the better and more accurate is the estimator. There is a universal pattern in all the true value settings and estimators that as the sample size ($n$) increases, both RMSE and bias decrease. This confirms the theoretical property that the greater the data utilized, the more precise are the parameter estimates. For instance, in the Table **1** with true parameters $s=0.05,k=0.75,\theta=0.2$, MLE of $s$ has 0.01243 of bias and 0.07021 of RMSE for $n=15$ but decrease significantly to 0.00158 and 0.01989, respectively, at $n=100$. Same for all the other estimators and parameters. The MLE generally has the smallest bias and RMSE for each of the estimators, especially for big

samples ( $n=100$ and $n=100$ ). This suggests that the MLE is the most efficient and unbiased estimator of the parameters of this distribution among those being considered. While other estimators like MPS and CvM could be as good or even marginally better for particular parameters at small sample sizes, the MLE performs the best at higher sample sizes. For example, at true values $s=0.07, k=0.80, \theta=0.35$ and $n=100$, the MLE of $\hat{\theta}$ is biased by 0.00779 and has an RMSE of 0.02833, both of which are lower than respective values for all other estimators. The LS, WLS, and MPS estimates have higher bias and RMSE, particularly at small sample sizes, and hence are less efficient under such conditions.

In Figure **3**, panels 9, 10, 11 and 12 respectively represents the plots of the bias and RMSE at sample sizes $n=15,25,75$ and $100$ for the respective true parameter settings. Notice that the behavior of the plots is consistent with conventional theory of asymptotic convergence, as the sample size becomes large, the RMSE decreases while the bias stays positive and relatively small. The implication is that the NGLTGE distribution is applicable in real life situations to model varying datasets.

## 6. GASP BASED ON TRUNCATED LIFE TESTS FOR NGLTGE MODEL

In quality control, acceptance sampling is a critical procedure for deciding whether to accept or reject a production lot based on a sample of items. While traditional single-item sampling plans can be time-consuming and costly, particularly for products with long lifetimes, the Group Acceptance Sampling Plan (GASP) offers an efficient alternative. GASP is a modern sampling technique that reduces the overall test time and cost by testing items in groups rather than

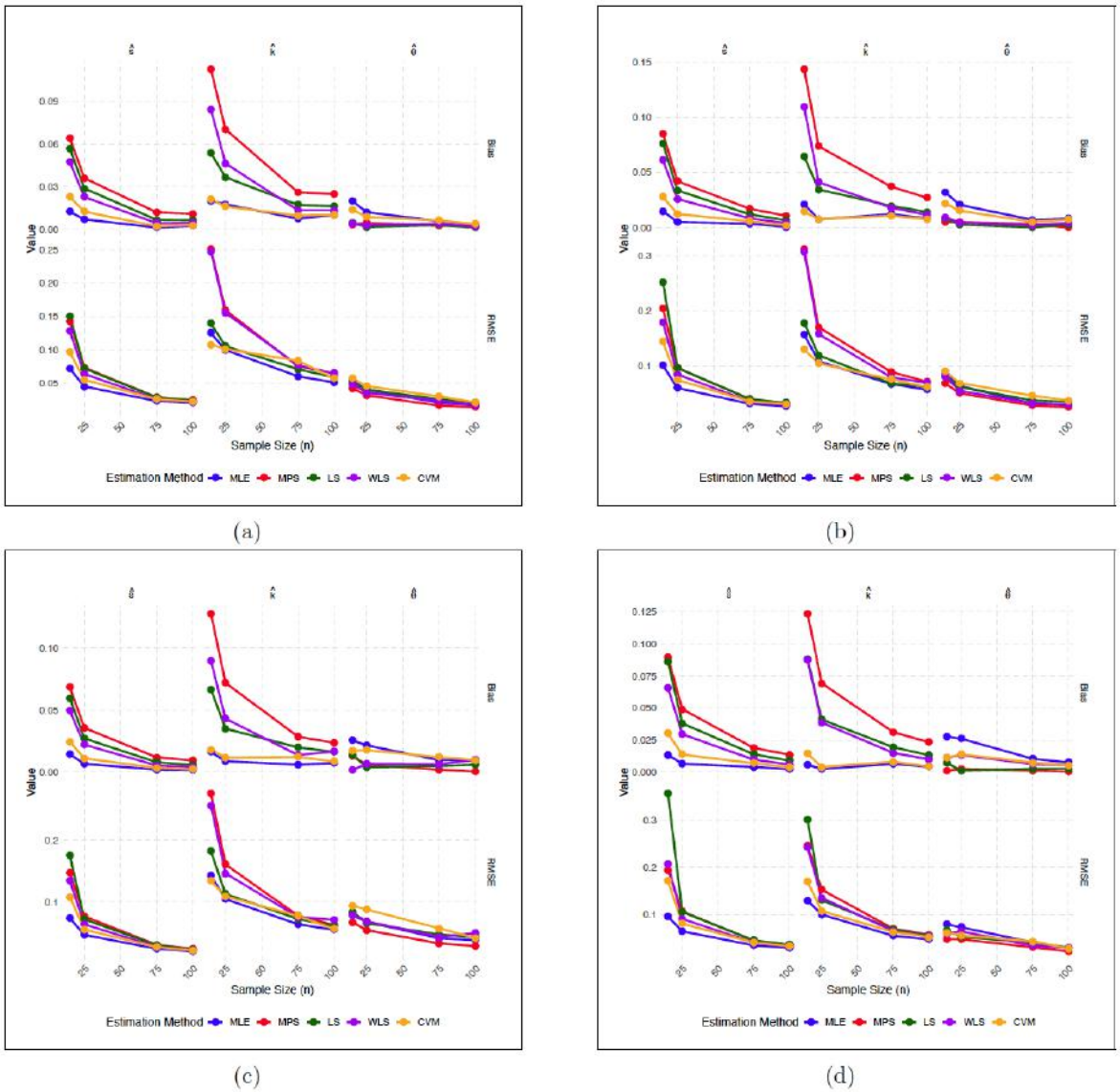


**Figure 3:** Plots of (**a**) Case I, (**b**) II, (**c**) III and (**d**) IV for Non-Bayesian Simulation Results.

individually. This approach is especially well-suited for reliability studies and truncated life tests, where the test is terminated at a pre-specified time ($t_0$) regardless of whether all units have failed.

This section presents the design of a GASP for the NGLTGE distribution under a truncated life test. We define the key parameters of the plan including the number of groups ($g$), the group size ($r$), and the acceptance number ($c$) by considering the median lifetime of the products. Our methodology is focused on minimizing the average sample number (ASN) while simultaneously satisfying the producer's and consumer's risk constraints. This optimization problem ensures that the sampling plan provides a statistically sound and cost-effective way to make lot acceptance decisions, thus balancing the interests of both the producer and the consumer. Recently, different distributions have been used to design GASP, see [37-40], The mathematical framework, including the derivation of the failure probability $p$ and the formulation of the acceptance probabilities, is detailed as follows;

Let the median lifetime be

$$\mu = \frac{k}{\theta}\log\left\{1+\frac{1}{s}\tan\left(\frac{\pi u}{2}\right)\right\}; \quad 0 \le u \le 1.$$

Define

$$\omega = k\log\left\{1+\frac{1}{s}\tan\left(\frac{\pi u}{2}\right)\right\},$$

so that for $u = 0.5 \quad \omega = \log\left\{1+\frac{1}{s}\tan\left(\frac{\pi}{4}\right)\right\}$. Therefore, we can write $\mu = \frac{\omega}{\theta}$.

In a truncated life testing scenario, the duration of the test is given as $t_0 = a_1 \times \mu_0$, where $a_1$ is a predetermined constant and $\mu_0$ is the hypothesized median lifetime. The ratio of the actual median lifetime to the hypothesized median lifetime is $r_2 = \frac{\mu}{\mu_0}$. The failure probability, $p$, of a single item before time $t_0$ is derived by inserting these relationships into the CDF of the NGLTGE distribution in Equation (2.3).

$$p = \frac{2}{\pi}\arctan\left\{s\exp\left(\frac{a_1 \times \omega}{kr_2}\right) - s\right\}$$

This expression for $p$ plays a crucial role in calculating the acceptance probabilities in the GASP scheme.

The GASP design parameters, i.e., the number of groups ($g$), the acceptance number ($c$), the group size ($r$), and the test duration ($t_0$), are determined such that both consumer and producer risks are balanced. For determining the optimal GASP design parameters, we formulate an optimization problem. We want to minimize the Average Sample Number (ASN), which is $c = r \times g$. This minimization is subject to the following, which balance consumer risk ($\beta$) and producer risk ($\alpha$):

$$P_{accept}(p_1 \mid \tfrac{\mu}{\mu_0} = r_1) = \left[\sum_{i=0}^{n}\binom{r}{i}p_1^i(1-p_1)^{r-i}\right]^g \le \beta, \qquad (6.1)$$

$$P_{accept}(p_2 \mid \tfrac{\mu}{\mu_0} = r_2) = \left[\sum_{i=0}^{n}\binom{r}{i}p_2^i(1-p_2)^{r-i}\right]^g \ge 1-\alpha. \qquad (6.2)$$

Here, $r_1$ and $r_2$ are the mean ratios relating to the consumer and producer risks, respectively. The failure probabilities $p_1$ and $p_2$ are calculated in these $P_{accept}$ functions, as provided in Equations (6.1) and (6.2).

Table **3** presents an illustrative set of GASP design parameters for the NGLTGE distribution, based on specific parameter values ($s = 0.5, k = 2.25$). The table shows the minimum required number of groups ($g$) and the acceptance number ($c$) for varying consumer risks ($\beta$), mean ratios ($\frac{\mu}{\mu_0}$), and test duration constants ($a_1$), for fixed group sizes ($r = 5$ and $r = 10$). The $P_{accept}(p)$ values indicate the probability of accepting a lot under these conditions.

Tables **3** and **4** give the performance of the GASP under the NGLTGE distribution, which aims to minimize the values of $g$ and $c$, which are the number of groups and acceptance number, respectively. The tables give the results for various values of $\beta$, the true mean $\mu$ to the specified mean $\mu_0$ ($\frac{\mu}{\mu_0}$), the number of groups $r$, and the coefficient $a_1$. The primary assessment criterion is the probability of acceptance ($P_{accept}(p)$). The results consistently show that as the ratio $\frac{\mu}{\mu_0}$ increases, the probability of acceptance is high, typically above 95% in most instances, demonstrating the effectiveness of the sampling plan in terms of accepting lots with or higher than the required mean life. Conversely, if the ratio is low, especially at $\frac{\mu}{\mu_0} = 2$, the plan will have zero groups ($g = 0$) and zero

**Table 3: GASP under NGLTGE at $s=0.5, k=2.25$ and with Minimum $g$ and $c$**

| $\beta$ | $\frac{\mu}{\mu_0}$ | $r=5$ | | | | | | $r=10$ | | | | | |
|---|---|---|---|---|---|---|---|---|---|---|---|---|---|
| | | $a_1=0.5$ | | | $a_1=1$ | | | $a_1=0.5$ | | | $a_1=1$ | | |
| | | **g** | **c** | $P_{accept}(p)$ | **g** | **c** | $P_{accept}(p)$ | **g** | **c** | $P_{accept}(p)$ | **g** | **c** | $P_{accept}(p)$ |
| 0.25 | 2 | 0 | 0 | – | 0 | 0 | – | 44 | 4 | 0.97582 | 73 | 4 | 0.960203 |
| | 4 | 18 | 2 | 0.982989 | 29 | 2 | 0.972736 | 2 | 2 | 0.983057 | 4 | 2 | 0.966401 |
| | 6 | 4 | 1 | 0.965478 | 29 | 2 | 0.992178 | 1 | 1 | 0.964301 | 4 | 2 | 0.990637 |
| | 8 | 4 | 1 | 0.980596 | 7 | 1 | 0.96629 | 1 | 1 | 0.9801 | 2 | 1 | 0.960595 |
| 0.10 | 2 | 0 | 0 | – | 0 | 0 | – | 0 | 0 | – | 0 | 0 | – |
| | 4 | 38 | 2 | 0.964427 | 449 | 3 | 0.989712 | 5 | 2 | 0.958179 | 23 | 3 | 0.989562 |
| | 6 | 38 | 2 | 0.989763 | 58 | 2 | 0.984417 | 5 | 2 | 0.98831 | 7 | 2 | 0.983672 |
| | 8 | 9 | 1 | 0.956869 | 58 | 2 | 0.993538 | 2 | 1 | 0.960595 | 7 | 2 | 0.99335 |
| 0.05 | 2 | 27 | 4 | 0.957196 | 204 | 5 | 0.970826 | 3 | 5 | 0.966688 | 13 | 6 | 0.977626 |
| | 4 | 3 | 2 | 0.971533 | 5 | 2 | 0.953007 | 1 | 3 | 0.987301 | 2 | 3 | 0.974763 |
| | 6 | 3 | 2 | 0.991337 | 5 | 2 | 0.985603 | 1 | 2 | 0.97786 | 1 | 2 | 0.97786 |
| | 8 | 2 | 1 | 0.959622 | 2 | 1 | 0.959622 | 1 | 2 | 0.990419 | 1 | 2 | 0.990419 |
| 0.01 | 2 | 266 | 5 | 0.962129 | 0 | 0 | – | 16 | 6 | 0.972534 | 25 | 6 | 0.957417 |
| | 4 | 17 | 3 | 0.986483 | 26 | 3 | 0.979402 | 2 | 3 | 0.974763 | 3 | 3 | 0.962384 |
| | 6 | 6 | 2 | 0.982748 | 10 | 2 | 0.971413 | 2 | 2 | 0.956211 | 2 | 2 | 0.956211 |
| | 8 | 6 | 2 | 0.992632 | 10 | 2 | 0.987751 | 2 | 2 | 0.980931 | 2 | 2 | 0.980931 |

**Table 4: GASP under NGLTGE at $s=1.25, k=0.25$ and with Minimum $g$ and $c$**

| $\beta$ | $\frac{\mu}{\mu_0}$ | $r=5$ | | | | | | $r=10$ | | | | | |
|---|---|---|---|---|---|---|---|---|---|---|---|---|---|
| | | $a_1=0.5$ | | | $a_1=1$ | | | $a_1=0.5$ | | | $a_1=1$ | | |
| | | **g** | **c** | $P_{accept}(p)$ | **g** | **c** | $P_{accept}(p)$ | **g** | **c** | $P_{accept}(p)$ | **g** | **c** | $P_{accept}(p)$ |
| 0.25 | 2 | 0 | 0 | – | 0 | 0 | – | 44 | 4 | 0.951891 | 0 | 0 | – |
| | 4 | 12 | 2 | 0.976062 | 20 | 2 | 0.960422 | 2 | 2 | 0.968604 | 12 | 3 | 0.987154 |
| | 6 | 3 | 1 | 0.956588 | 20 | 2 | 0.988114 | 2 | 2 | 0.990491 | 4 | 2 | 0.981072 |
| | 8 | 3 | 1 | 0.975191 | 5 | 1 | 0.958995 | 1 | 1 | 0.967642 | 4 | 2 | 0.991956 |
| 0.10 | 2 | 0 | 0 | – | 0 | 0 | – | 0 | 0 | – | 0 | 0 | – |
| | 4 | 172 | 3 | 0.989105 | 264 | 3 | 0.983326 | 15 | 3 | 0.983968 | 23 | 3 | 0.975523 |
| | 6 | 26 | 2 | 0.984576 | 40 | 2 | 0.97637 | 5 | 2 | 0.976397 | 7 | 2 | 0.967112 |
| | 8 | 26 | 2 | 0.993473 | 40 | 2 | 0.989975 | 5 | 2 | 0.989955 | 7 | 2 | 0.985965 |
| 0.05 | 2 | 61 | 5 | 0.970205 | 101 | 5 | 0.951151 | 721 | 6 | 0.972205 | 0 | 0 | – |
| | 4 | 6 | 3 | 0.98752 | 9 | 3 | 0.981338 | 11 | 3 | 0.977239 | 17 | 3 | 0.965043 |
| | 6 | 3 | 2 | 0.981606 | 4 | 2 | 0.975551 | 5 | 2 | 0.969532 | 7 | 2 | 0.957607 |
| | 8 | 1 | 1 | 0.966008 | 4 | 2 | 0.989238 | 5 | 2 | 0.986565 | 7 | 2 | 0.981242 |
| 0.01 | 2 | 8 | 6 | 0.967281 | 41 | 7 | 0.97932 | 54 | 7 | 0.972853 | 82 | 7 | 0.959068 |
| | 4 | 1 | 3 | 0.973006 | 3 | 4 | 0.986994 | 4 | 4 | 0.982697 | 5 | 4 | 0.978418 |
| | 6 | 1 | 2 | 0.958029 | 1 | 2 | 0.958029 | 2 | 3 | 0.987659 | 3 | 3 | 0.981545 |
| | 8 | 1 | 2 | 0.98075 | 1 | 2 | 0.98075 | 2 | 2 | 0.961871 | 2 | 2 | 0.961871 |

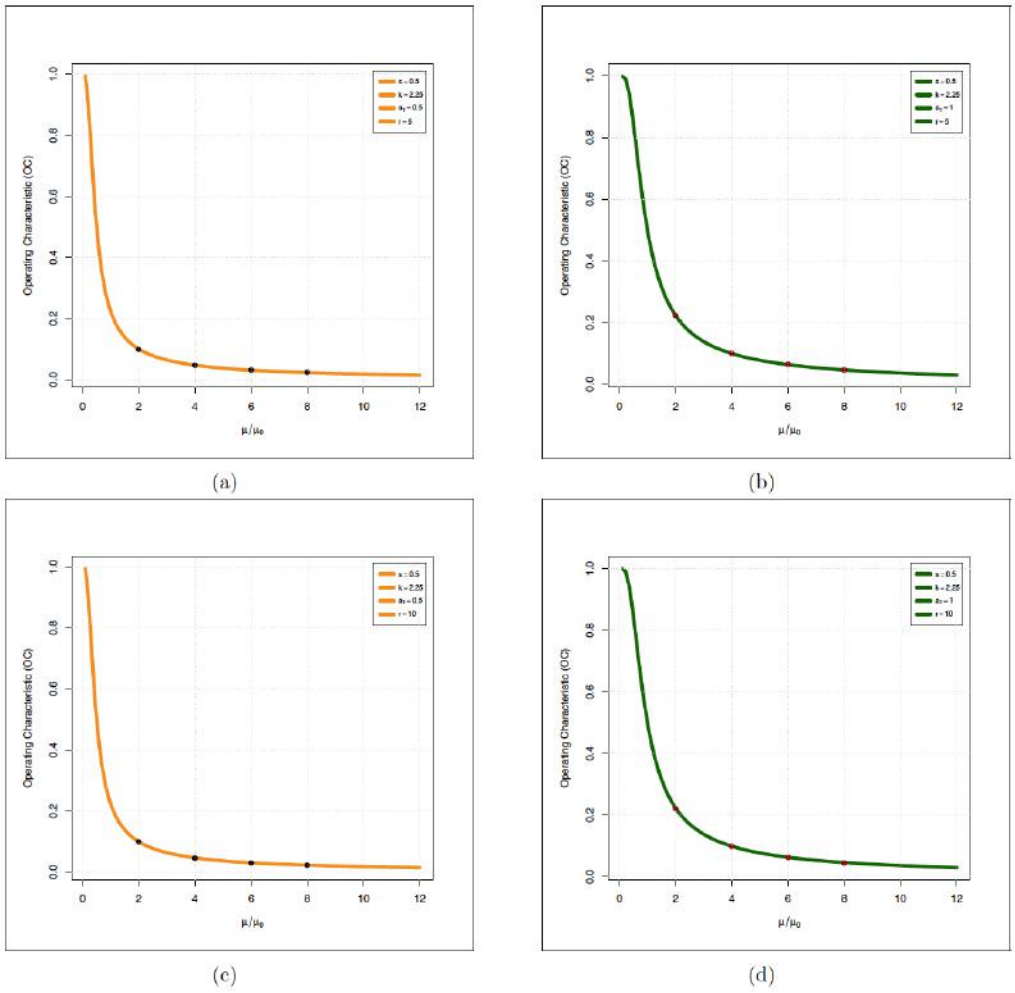


**Figure 4:** OC Curve for $s=0.5, k=2.25$.

acceptance numbers ($c=0$), hence giving an indeterminate or undefined acceptance probability. It is clear at the lowest levels of $\beta$ (0.10 and 0.25). A major discovery is that the $g$ and $c$ values simply rely on the number of groups ($r$) and on the coefficient $a_1$. For a fixed $\beta$ and $\frac{\mu}{\mu_0}$, increasing $r$ from 5 to 10 will generally give smaller $g$ and $c$, and generally also a small increase in the probability of acceptance. Similarly, increasing $a_1$ from 0.5 to 1 will generally give larger $g$ and $c$, with negligible impact on the probability of acceptance. Minimum values of $g$ and $c$ will be obtained when the ratio $\frac{\mu}{\mu_0}$ is maximum, showing that if the actual mean life is much greater than the assigned mean, lower number of groups and smaller acceptance number will be required to ensure high probability of acceptance.

Figure **4** is the Operating Characteristic (OC) curve for $s=0.5, k=2.25$. In panel 14 is when $r=5$ and $a_1=0.5$, panel 15 is when $r=5$ and $a_1=1$, panel 16 is when $r=10$ and $a_1=0.5$, panel 17 is when $r=10$ and $a_1=1$.

Figure **5** is the Operating Characteristic (OC) curve for $s=1.25, k=0.25$. In panel 19 is when $r=5$ and $a_1=0.5$, panel 20 is when $r=5$ and $a_1=1$, panel 21 is when $r=10$ and $a_1=0.5$, panel 22 is when $r=10$ and $a_1=1$.

## 7. NUMERICAL ANALYSIS

The first application is the weekly volume of traded bitcoin-usd from 17/09/2023 to 15/9/2024 in 1,000,000, 000.

The second application focuses on the COVID-19 death rate for Angola from 14/06/2020 to 20/2/2022.

The third data set represents the survival times (in months) for 121 breast cancer patients treated between 1929 and 1938. It was first reported by lawless [41] statistical and presented in Table

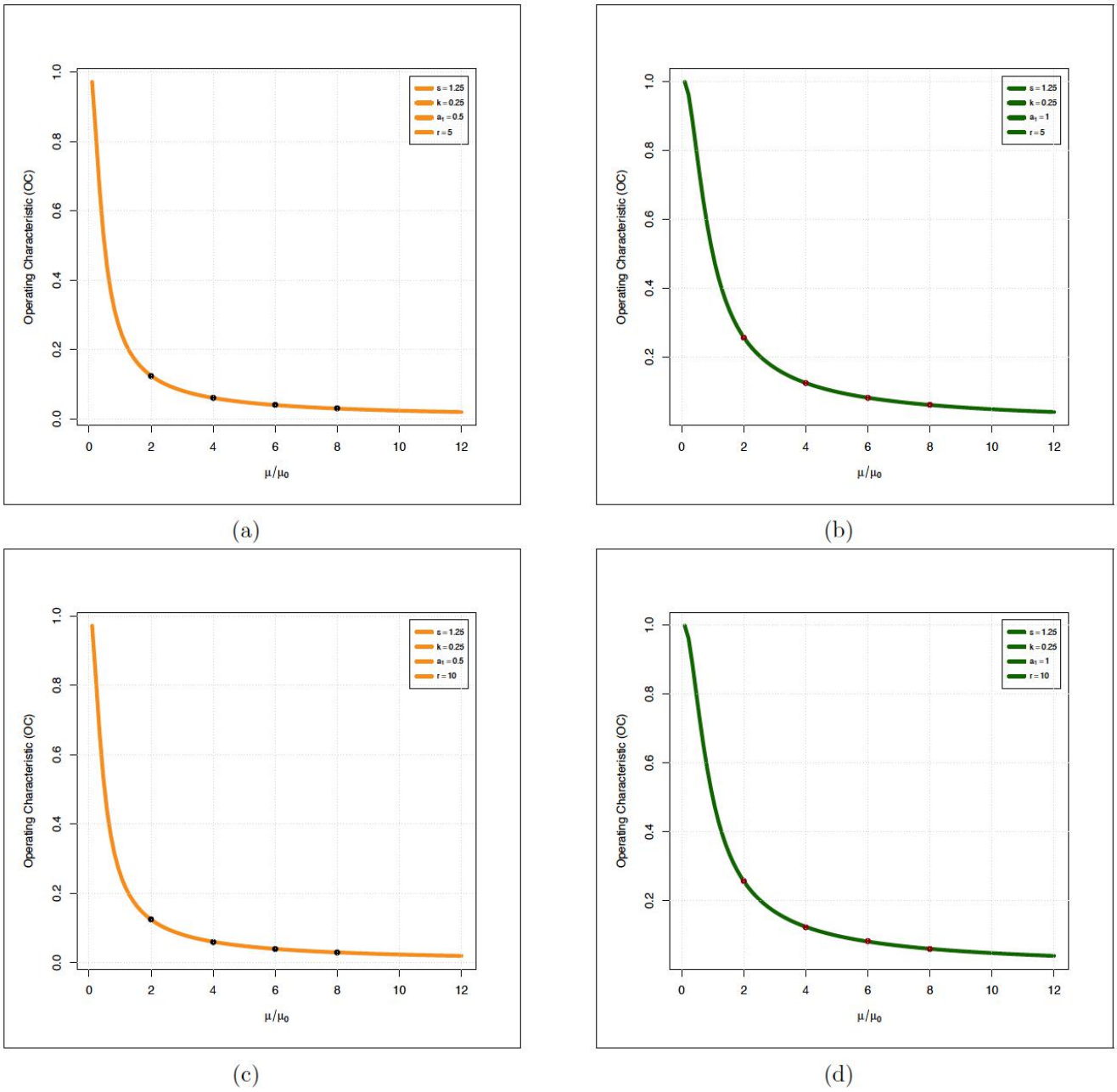


**Figure 5:** OC Curve for $s = 1.25, k = 0.25.$

**Table 5: Weekly Volume of Traded Bitcoin-USD**

| | | | | | | |
|---|---|---|---|---|---|---|
| 0.256559779 | 0.822519052 | 0.730122407 | 0.821837757 | 0.726736545 | 1.134023831 | 1.65718773 |
| .155200566 | 1.347674948 | 1.435353611 | 1.30439894 | 1.34360108 | 1.885036149 | 1.68493482 |
| .520841715 | 1.578071262 | 2.02311774 | 2.599718197 | 1.391358248 | 1.553146029 | 1.351841874 |
| .578263954 | 2.135600415 | 1.607691456 | 3.228956661 | 4.057096933 | 4.059577506 | 3.280971217 |
| .163246258 | 2.294272601 | 2.882436754 | 2.578895559 | 1.760310882 | 2.177170118 | 1.616178571 |
| .91456349 | 2.25779718 | 1.709494099 | 1.875695007 | 1.759732716 | 1.634490154 | 1.710300939 |
| .131075314 | 1.8740702 | 2.221618762 | 2.27265185 | 2.510023388 | 3.171587346 | 1.937313931 |
| .006702741 | 2.085891553 | 2.070528442 | 1.832794312 | | | |

**Table 6: COVID-19 Death Rate for Angola**

| | | | | | | | |
|---|---|---|---|---|---|---|---|
| 0.0588235 | 0.0229885 | 0.1034483 | 0.0437956 | 0.0196078 | 0.0436681 | 0.0604839 | 0.0392157 |
| .0521173 | 0.0313725 | 0.0311751 | 0.0260417 | 0.0375000 | 0.0265018 | 0.0285344 | 0.0272206 |
| .0376712 | 0.0189145 | 0.0166240 | 0.0095559 | 0.0104575 | 0.0182868 | 0.0134745 | 0.0133531 |
| .0200445 | 0.0192000 | 0.0430108 | 0.0267686 | 0.0152505 | 0.0164234 | 0.0246305 | 0.0431894 |
| .0168675 | 0.0392857 | 0.0599251 | 0.0411765 | 0.0282686 | 0.0219780 | 0.0298507 | 0.0160858 |
| .0208955 | 0.0127737 | 0.0132979 | 0.0113519 | 0.0134228 | 0.0173847 | 0.0180505 | 0.0133191 |
| .0334262 | 0.0206795 | 0.0261669 | 0.0308151 | 0.0308765 | 0.0335498 | 0.0357143 | 0.0267983 |
| .0302663 | 0.0272109 | 0.0278578 | 0.0404908 | 0.0446334 | 0.0420561 | 0.0412044 | 0.0472779 |
| .0368393 | 0.0311383 | 0.0397910 | 0.0228466 | 0.0166540 | 0.0284974 | 0.0334686 | 0.0217028 |
| .0392857 | 0.0326531 | 0.0267857 | 0.0234375 | 0.0190476 | 0.0130719 | 0.0021231 | 0.0015169 |
| .0023099 | 0.0058021 | 0.0101074 | 0.0121951 | 0.0037123 | 0.0068027 | 0.0122699 | 0.0097087 |

**Table 7: Breast Cancer Patients Survival Times**

| | | | | | | | | | | | | | | |
|---|---|---|---|---|---|---|---|---|---|---|---|---|---|---|
| 0.3 | 0.3 | 4 | 5 | 5.6 | 6.2 | 6.3 | 6.6 | 6.8 | 7.4 | 7.5 | 8.4 | 8.4 | 10.3 | 11 |
| .8 | 12.2 | 12.3 | 13.5 | 14.4 | 14.4 | 14.8 | 15.5 | 15.7 | 16.2 | 16.3 | 16.5 | 16.8 | 17.2 | 17.3 |
| .5 | 17.9 | 19.8 | 20.4 | 20.9 | 21 | 21 | 21.1 | 23 | 23.4 | 23.6 | 24 | 24 | 27.9 | 28.2 |
| .1 | 30 | 31 | 31 | 32 | 35 | 35 | 37 | 37 | 37 | 38 | 38 | 38 | 39 | 39 |
| | 40 | 40 | 41 | 41 | 41 | 42 | 43 | 43 | 43 | 44 | 45 | 45 | 46 | 46 |
| | 48 | 49 | 51 | 51 | 51 | 52 | 54 | 55 | 56 | 57 | 58 | 59 | 60 | 60 |
| | 61 | 62 | 65 | 65 | 67 | 67 | 68 | 69 | 78 | 80 | 83 | 88 | 89 | 90 |
| | 96 | 103 | 105 | 109 | 109 | 111 | 115 | 117 | 125 | 126 | 127 | 129 | 129 | 139 |

**Table 8: Summary of Basic Statistics**

| Statistics | Data I | Data II | Data III |
|---|---|---|---|
| $n$ | 53 | 88 | 121 |
| $Q_1$ | 0.1520842 | 0.016339 | 17.5 |
| $Q_3$ | 0.217717 | 0.03599555 | 60 |
| IQR | 0.06563284 | 0.01965655 | 42.5 |
| | 0.02565598, 0.3228957 | | 125, 126, 127 |
| Outlier | 0.4057097, 0.4059578, | 0.1034483 | 129, 129, 139 |
| | 0.3280971, 0.3171587 | | 154 |
| Mean | 0.1900383 | 0.0268645 | 46.32893 |
| Median | 0.1832794 | 0.02633435 | 40 |
| Variance | 0.005644836 | 0.000246428 | 1244.464 |
| Standard Deviation | 0.07513212 | 0.01569803 | 35.27697 |
| Range | 0.38030182 | 0.1019314 | 153.7 |
| Skewness | 0.7768817 | 1.477419 | 1.04318 |
| Kurtosis | 4.267464 | 8.012109 | 3.402139 |

**Table 9: Model Evaluation Measures**

| Data | Distribution | LL | AIC | CAIC | BIC | HQIC | W | A | KS | p-value |
|---|---|---|---|---|---|---|---|---|---|---|
| Data I | NGLTGE | 66.78 | -125.5512 | -125.0614 | -119.6403 | -123.2781 | 0.0517 | 0.3558 | 0.0650 | 0.9677 |
| | NGLXTE | 61.05 | -118.1091 | -117.8691 | -114.1685 | -116.5937 | 0.2191 | 1.2936 | 0.1550 | 0.1407 |
| | APWQ | 63.07 | -120.1605 | -119.6707 | -114.2496 | -117.8875 | 0.1503 | 0.8985 | 0.1294 | 0.3101 |
| | LTW | 63.03 | -118.9463 | -118.1129 | -111.0651 | -115.9155 | 0.1400 | 0.8787 | 0.1315 | 0.2919 |
| | LW | 63.46 | -120.9195 | -120.4297 | -115.0086 | -118.6464 | 0.1040 | 0.6590 | 0.0867 | 0.7880 |
| Data II | NGLTGE | 251.05 | -496.1013 | -495.8156 | -488.6693 | -493.1071 | 0.0372 | 0.2699 | 0.0515 | 0.9738 |
| | NGLXTE | 243.86 | -483.7146 | -483.5734 | -478.7599 | -481.7185 | 0.1097 | 0.8680 | 0.1055 | 0.2809 |
| | APWQ | 249.40 | -492.9296 | -492.6439 | -485.4976 | -489.9354 | 0.0461 | 0.4167 | 0.0607 | 0.9015 |
| | LTW | 250.31 | -492.6203 | -492.1384 | -482.7109 | -488.6281 | 0.0497 | 0.4220 | 0.0698 | 0.7852 |
| | LW | 245.39 | -489.7755 | -484.4898 | -477.3435 | -481.7813 | 0.1757 | 1.1997 | 0.0860 | 0.5325 |
| Data III | NGLTGE | -579.66 | 1165.3210 | 1165.5270 | 1173.7090 | 1168.7280 | 0.0553 | 0.4272 | 0.0583 | 0.8059 |
| | NGLXTE | -580.25 | 1164.5000 | 1164.6020 | 1170.0920 | 1166.7710 | 0.1434 | 0.9557 | 0.0799 | 0.4233 |
| | APWQ | -579.26 | 1164.6410 | 1164.2460 | 1172.4280 | 1167.4470 | 0.0540 | 0.4064 | 0.0584 | 0.8036 |
| | LTW | -591.40 | 1170.6950 | 1171.0400 | 1181.8780 | 1175.2370 | 0.1410 | 0.8005 | 0.1337 | 0.0264 |
| | LW | -587.60 | 1181.1990 | 1181.4040 | 1189.5870 | 1184.6060 | 0.2097 | 1.2578 | 0.0936 | 0.2391 |

Table **8** provides a statistical overview of the three distinct datasets, Data I, Data II, and Data III, reporting their central tendency, dispersion, and shape. Data I has a sample size of $n = 53$, mean of approximately 0.190 and median 0.183, showing a moderate positive skew. Having a variance of 0.0056 and standard deviation of 0.075, it has a relatively small spread of values. This is also indicated by the 0.777 skewness and 4.267 kurtosis, suggesting a heavier-than-normal distribution with more than one outlier. For Data II, $n = 88$, the mean is 0.0269 and the median 0.0263. The 1.477 skewness and 8.012 kurtosis are both extremely high, indicating a strong positive skew and an extremely leptokurtic distribution with a more extreme peak and heavier tails than a normal distribution. The 0.00025 variance and 0.0157 standard deviation, along with the narrow Interquartile Range (IQR) of 0.0197, illustrate that the data values are clustered together. The single outlier at 0.1034 is distant from the body of data. Data III, which has the largest number of data at $n = 121$, is the most dispersed. Its mean at 46.33 and median at 40 are widely separated, and the large skewness of 1.043 indicates high positive skew. The variance of 1244.46 and standard deviation of 35.28 are considerably larger than those of the other two datasets, suggesting a wide spread of values. The kurtosis of 3.402 is close to that of a normal distribution. A number of outliers, from 125 to 154, also explain the big range of 153.7. Overall, each dataset exhibits a different set of features, including Data III being the most spread out, Data II the most compact and most skewed, and Data I intermediate in dispersion.

Table **9** provides a comprehensive comparison of the fit of five statistical distributions NGLTGE, NGLXTE, APWQ, LTW, and LW to three data sets: Data I, Data II, and Data III. The models are compared according to various criteria, including LL, AIC, CAIC, Bayesian Information Criterion (BIC), and Hannan-Quinn Information Criterion (HQIC). The analysis suggests that smaller values of these information criteria indicate a better-fitting model. Goodness-of-fit is also assessed by Anderson-Darling (W, A) and Kolmogorov-Smirnov (KS) statistics, where a large p-value of the KS test shows that the data likely meet the specified distribution. For Data I, the NGLTGE distribution gives the best fit. It has the highest log-likelihood (LL = 66.78) and the lowest values of all information criteria (AIC = -125.5512, CAIC = -125.0614, BIC = -119.6403, HQIC = -123.2781). Additionally, its Kolmogorov-Smirnov (KS) statistic of 0.0650 is the lowest and its p-value of 0.9677 is the highest, providing strong evidence that NGLTGE is the most appropriate model for this data. For Data II, the NGLTGE distribution once more offers the best fit. It has the highest log-likelihood (LL = 251.05) and the lowest information criteria values. Its KS p-value of 0.9738 is the largest of all the models, which further confirms its adequacy. Even though the APWQ distribution also has a high p-value (0.9015), the NGLTGE model is much better due to having lower values of the information criteria. For Data III, the NGLTGE distribution is once again the best-fitting model. Although the LL is negative (-579.66), it is the highest, and the information criteria (AIC = 1165.3210, CAIC = 1165.5270, BIC = 1173.7090, HQIC = 1168.7280) are the lowest. The KS p-value 0.8059 is

**Table 10: Parameter Estimates for the Fitted Models**

| Data | Distribution | MLEs (Standard Errors) | | | |
|---|---|---|---|---|---|
| Data I | NGLTGE | $\hat{s}$ 0.0232(0.0131) | $\hat{k}$ 0.0963(0.2047) | $\hat{\theta}$ 1.9881(4.2374) | |
| | NGLXTE | $\hat{a}$ 0.5289(0.0555) | $\hat{l}$ 3.1585(0.1713) | | |
| | APWQ | $\hat{\alpha}$ 2.4949(4.4809) | $\hat{\beta}$ 2.9698(0.7018) | $\hat{\lambda}$ 72.6897(41.1816) | |
| | LTW | $\hat{s}$ 1.7196(1.0183) | $\hat{k}$ 0.1832(0.0305) | $\hat{a}$ 0.1118(0.0010) | $\hat{b}$ 2.8109(0.0013) |
| | LW | $\hat{a}$ 1.0860(–) | $\hat{b}$ 6.4300(–) | $\hat{l}$ 4.0575(–) | |
| Data II | NGLTGE | $\hat{s}$ 0.1484(0.0541) | $\hat{k}$ 0.0428(0.0543) | $\hat{\theta}$ 3.4920(4.4711) | |
| | NGLXTE | $\hat{a}$ 0.8234(0.0678) | $\hat{l}$ 21.2834(1.3384) | | |
| | APWQ | $\hat{\alpha}$ 0.3171(0.6273) | $\hat{\beta}$ 1.6163(0.2867) | $\hat{\lambda}$ 383.7133(233.1578) | |
| | LTW | $\hat{s}$ 0.0753(0.3791) | $\hat{k}$ 5.8251(5.1657) | $\hat{a}$ 0.2958(0.7065) | $\hat{b}$ 2.0415(0.2516) |
| | LW | $\hat{a}$ 0.3908(5.3189) | $\hat{b}$ 4.3174(85.9392) | $\hat{l}$ 6.9070(93.9956) | |
| Data III | NGLTGE | $\hat{s}$ 0.5821(0.1769) | $\hat{k}$ 1.7354(3.8367) | $\hat{\theta}$ 0.0458(0.1009) | |
| | NGLXTE | $\hat{a}$ 1.0443(0.0805) | $\hat{l}$ 0.0125(0.0008) | | |
| | APWQ | $\hat{\alpha}$ 0.8709(0.5828) | $\hat{\beta}$ 1.2865(0.0758) | $\hat{\lambda}$ 0.0068(0.0028) | |
| | LTW | $\hat{s}$ 9.9149(4.6474) | $\hat{k}$ 0.1008(0.0103) | $\hat{a}$ 2.3466(0.0049) | $\hat{b}$ 0.8683(0.0043) |
| | LW | $\hat{a}$ 0.7676(0.7618) | $\hat{b}$ 0.0650(0.1763) | $\hat{l}$ 2.4179(2.4089) | |

the highest, indicating a good fit. For comparison, the LTW model to Data III has a very low KS p-value (0.0264), indicating that it is not a good fit for this data. Concisely, the NGLTGE distribution provides the best fit to all three datasets on every evaluation measure used, ranging from log-likelihood to information criteria and goodness-of-fit tests.

Table **10** displays the Maximum Likelihood Estimates (MLEs) and standard errors of the parameters of five distributions that were fitted to three data sets. Standard errors are an indication of the estimates' accuracy, with lower values indicating more precise parameter estimates. For Data I, the NGLTGE distribution provides the parameter estimates $\hat{s} = 0.0232$, $\hat{k} = 0.0963$, and $\hat{\theta} = 1.9881$. The standard errors of $\hat{k}$ and $\hat{\theta}$ are especially large, indicating great variability in estimating them. The NGLXTE and LTW models, however, have relatively small standard errors for respective parameters, indicating better estimates. APWQ and LW models also have parameters with large standard errors, notably $\hat{\alpha}$, $\hat{\lambda}$ and all the parameters of the LW model. In Data II, the NGLTGE model is estimating parameters with varying degrees of precision. $\hat{s}$ has a fairly precise estimate (standard error of 0.0541), while estimates of $\hat{k}$ and $\hat{\theta}$ both have much greater standard errors, specifically $\hat{\theta}$ with a standard error of 4.4711. The NGLXTE model again has very precise estimates, with the standard errors for $\hat{a}$ and $\hat{l}$ both small. The APWQ, LTW, and LW models all possess great standard errors for the majority of their parameters, indicating these parameter estimates are less reliable. Finally, within Data III, the NGLTGE model contains estimates with mixed precision. The

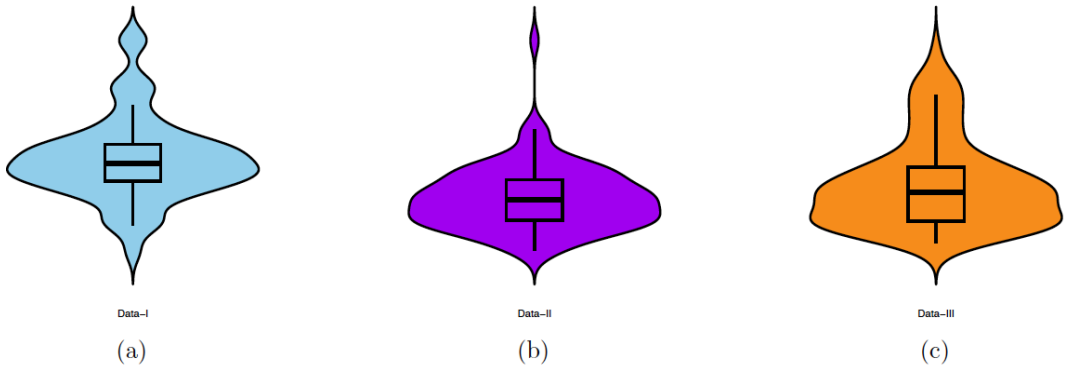


**Figure 6:** Boxplot superimposed on Violin plot for (**a**) Data I, (**b**) Data II, (**c**) Data III.

standard error for $\hat{s}$ is small in magnitude (0.1769), while the standard errors for $\hat{k}$ and $\hat{\theta}$ are larger. As in the case with the other datasets, the NGLXTE model for Data III is characterized by extremely accurate parameter estimates, with standard errors of 0.0805 for $\hat{a}$ and 0.0008 for $\hat{l}$. The other distributions (APWQ, LTW, LW) tend to have parameters with greater standard errors, though the LTW model's $\hat{k}$ and the APWQ model's $\hat{\beta}$ are estimated more accurately. Generally, although the NGLTGE distribution was previously mentioned to be most information-criteria and goodness-of-fit favorable, the NGLXTE distribution is always providing the best parameter estimates with all three datasets, as evident from its analysis with smaller standard errors of the parameters. This shows that although NGLTGE may be a better fitting for the overall shape of the data, the parameters of the NGLXTE model are better estimated and robust.

The plots in Figure **6** show the distributions of three datasets. Panel 24, has a fairly symmetric distribution with the median near the center of the box, and a few minor density peaks. Panel 25 is highly right-skewed, indicated by a long upper tail, a median positioned low in the box, and a dense concentration of data at the lower end of the range. Panel 26 also exhibits right-skewness, but with a much wider spread than the other two datasets, shown by the broader violin plot and larger box, and a median situated in the lower half of its box.

The provided TTT (Total Time on Test) plots in Figure **7** are used to assess the shape of the hazard rate of a distribution. The plots show the relationship between $T(i/n)$, the TTT plot function, and $i/n$, the empirical cumulative distribution. In panel 28, the TTT plot for Data I is concave, indicating that the distribution has an increasing hazard rate (IHR). This suggests that the risk of an event occurring increases over time. For panel 29, the TTT plot for Data II is also concave. This indicates an increasing hazard rate (IHR) for this dataset as well, similar to Data I. In panel 30, the TTT plot for Data III is a straight line, which suggests that the distribution has a constant hazard rate. This implies that the risk of an event is uniform over time.

Figure **8** show how well different distributions fit three datasets. In panel 32, for Data I, the NGLTGE distribution, shown in red, provides the closest fit to the histogram's shape compared to the other distributions. In panel 33, for Data II, the NGLTGE distribution again

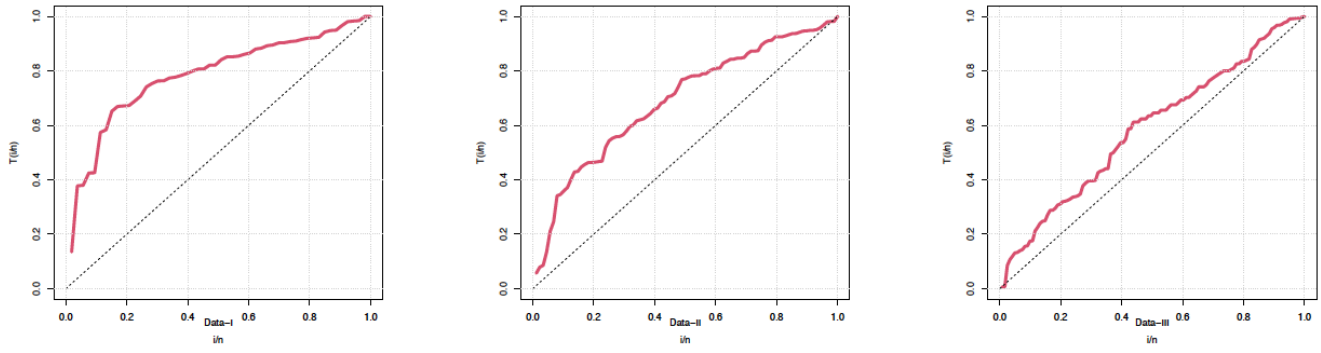


**Figure 7:** TTT plots for (a) Data I, (b) Data II, (c) Data III.

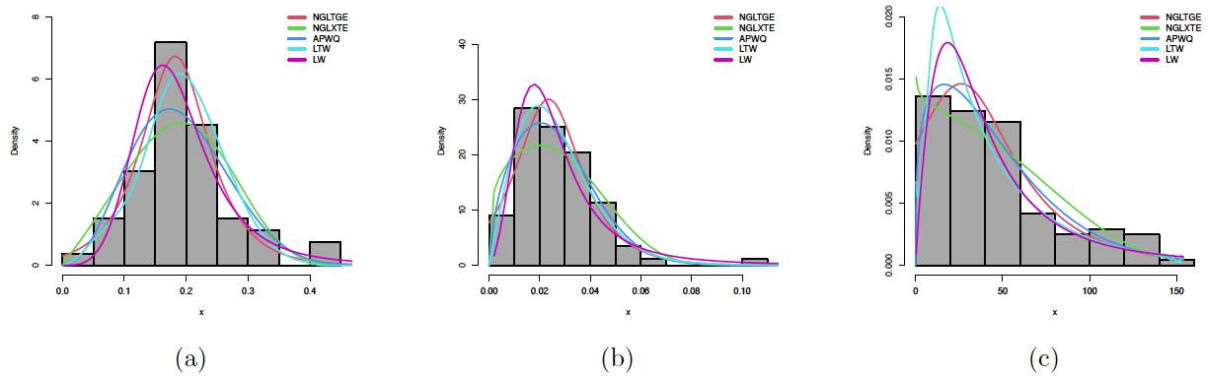


**Figure 8:** Density plot superimposed on Histogram for (**a**) Data I, (**b**) Data II, (**c**) Data III.

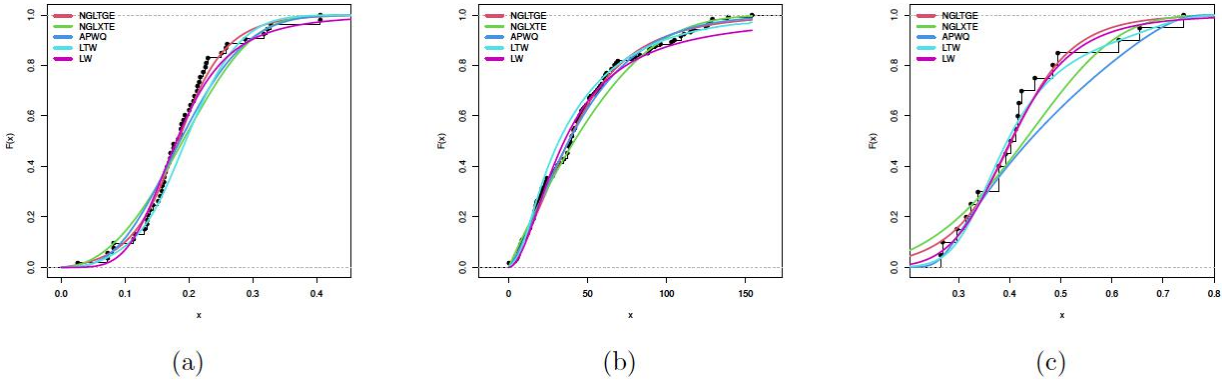


**Figure 9:** CDF plots for (**a**) Data I, (**b**) Data II, (**c**) Data III.

appears to be the best fit, closely following the high peak and the long tail of the data. For panel 34, Data III, the NGLTGE and APWQ distributions both provide a good fit to the histogram, with the NGLTGE line tracking the overall shape of the bars quite well.

Figure **9** compare the empirical cumulative distribution function (CDF) of the data with the theoretical CDFs of five fitted distributions. A good fit is indicated by the theoretical curve closely following the step-like empirical curve. In panel 36, for Data I, the NGLTGE distribution (red line) provides a very close fit to the empirical CDF, aligning well with the black dots that represent the data. In panel 37, for Data II, the theoretical curves for NGLTGE (red), APWQ (green), and LTW (blue) all appear to fit the empirical CDF well, showing that they are all suitable models for this dataset. In panel 38, for Data III, the NGLTGE (red) and LTW (blue) curves closely match the empirical CDF of the data, indicating a better fit compared to the other distributions.

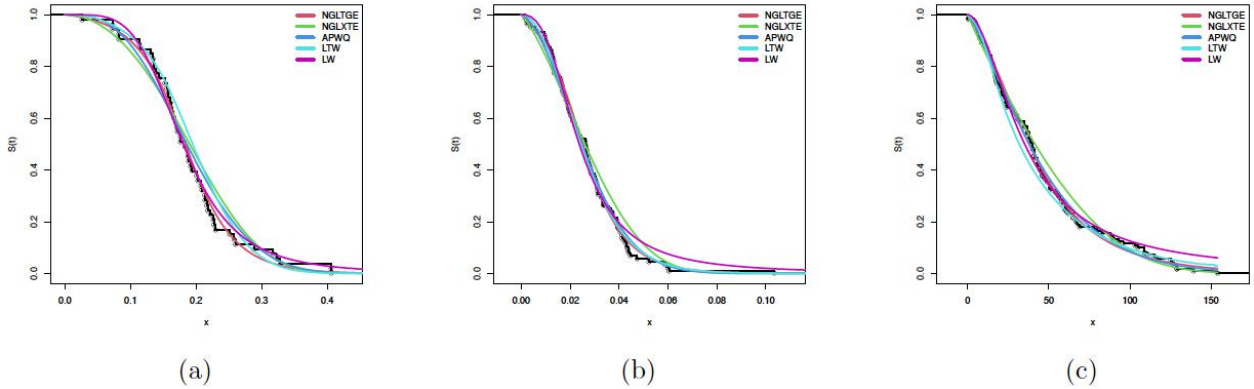


**Figure 10:** SF plots for (**a**) Data I, (**b**) Data II, (**c**) Data III.

Figure **10** compare the fitted survival functions (SFs) with the empirical survival function of the data. The survival function, $S(t)$, represents the probability of an item surviving beyond time $t$. A good fit is indicated by a theoretical curve that closely follows the empirical step-wise curve. In panel 40, for Data I, the NGLTGE distribution (red line) provides the best fit, closely tracking the empirical survival function across the entire range of data. In panel 41, for Data II, the NGLTGE distribution again appears to be the best fit, as its curve aligns most closely with the empirical plot, particularly in the initial, steep drop-off phase. In panel 42, for Data III, the NGLTGE and NGLXTE distributions are the most suitable, as their curves closely match the empirical data points, showing a good fit for this dataset as well. The other models do not capture the shape of the empirical data as accurately.

Figures **11**, **12**, and **13** are the Probability-Probability (P-P) plots for Data I, II and III respectively. Figures **14**, **15**, and **16** represent the Quantile-Quantile (Q-Q) plots for Data I, II and III respectively.

## 8. MACHINE LEARNING PERSPECTIVE

From a machine learning perspective, the proposed NGLTGE distribution can be understood as a parametric density estimator that balances parsimony, interpretability, and predictive performance. While much of the recent literature in probabilistic modeling has shifted toward highly flexible nonparametric or neural network-based density estimators, such as Gaussian mixtures [42], variational autoencoders [43], and normalizing flows [44], there remains strong value in developing new closed-form families with tractable likelihoods.

### 8.1. PyTorch Implementation

We fit the NGLTGE parameters $(s,k,\theta)$ by maximum likelihood in PyTorch [45]. The negative log-likelihood is differentiated using autograd and minimized with the Adam optimizer [46], removing the need to derive or solve score equations analytically. To enforce positivity and improve conditioning, we optimize unconstrained variables passed through a *softplus* transform to obtain $(s,k,\theta)>0$. For numerical stability we (i) rescale inputs by the empirical 95th percentile, (ii) clamp the argument of the exponential to avoid overflow, and (iii) clip gradients at a fixed norm.

Training uses double precision (float64) and reproducible seeds. Hyperparameters (learning rate, iterations, and optional mini-batch size) are tuned by

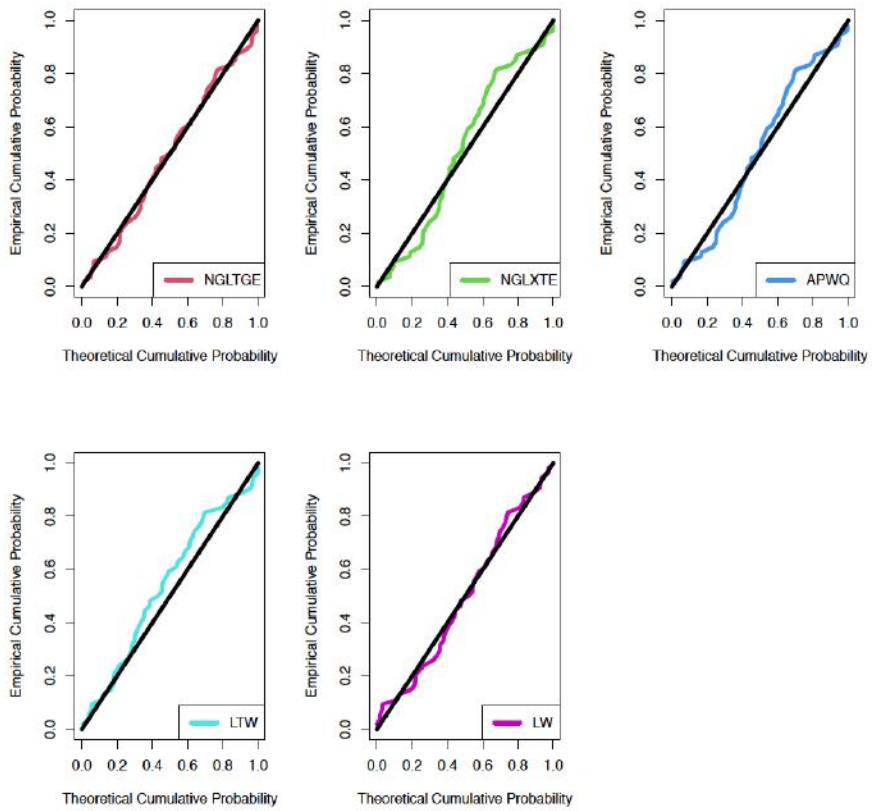


**Figure 11:** P-P plots for Data I.

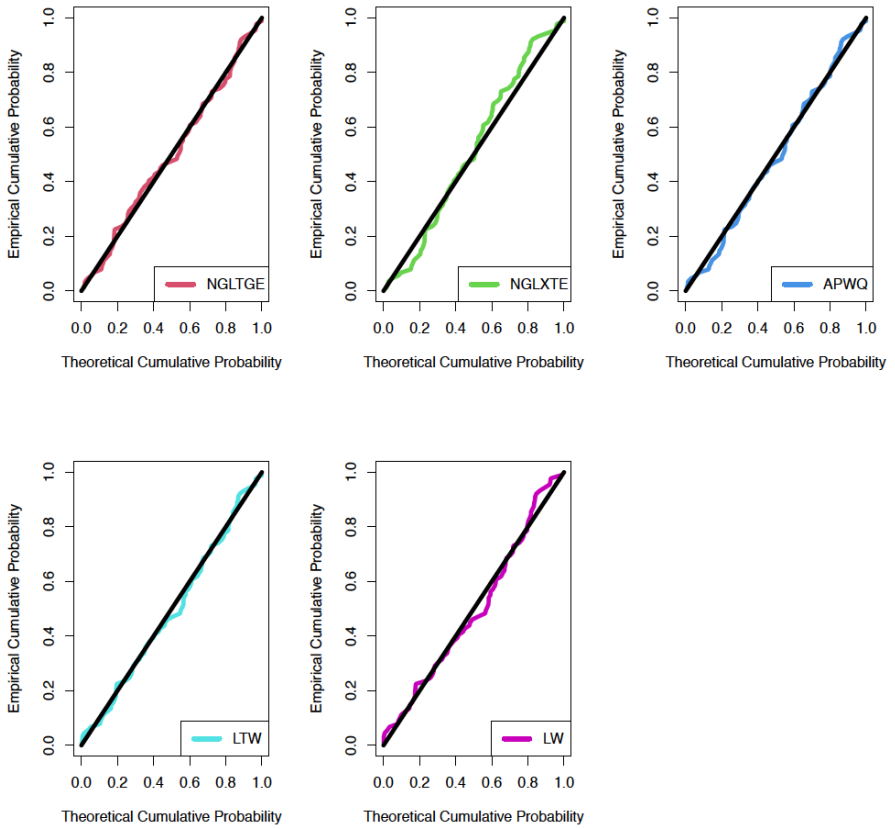


**Figure 12:** P-P plots for Data II.

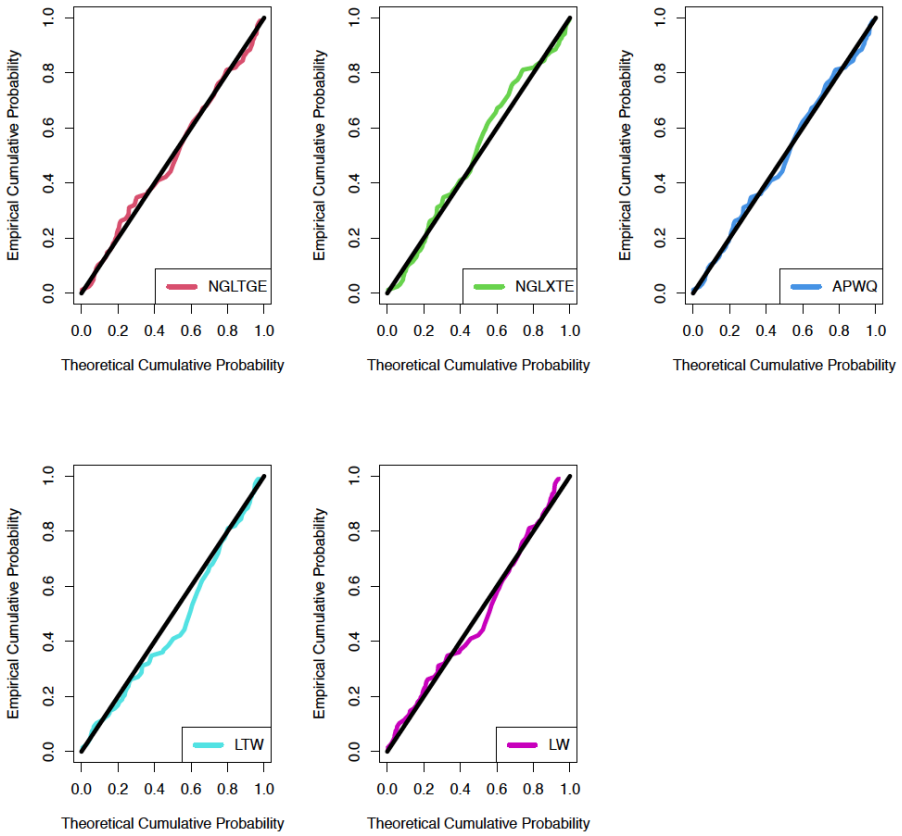


**Figure 13:** P-P plots for Data III.

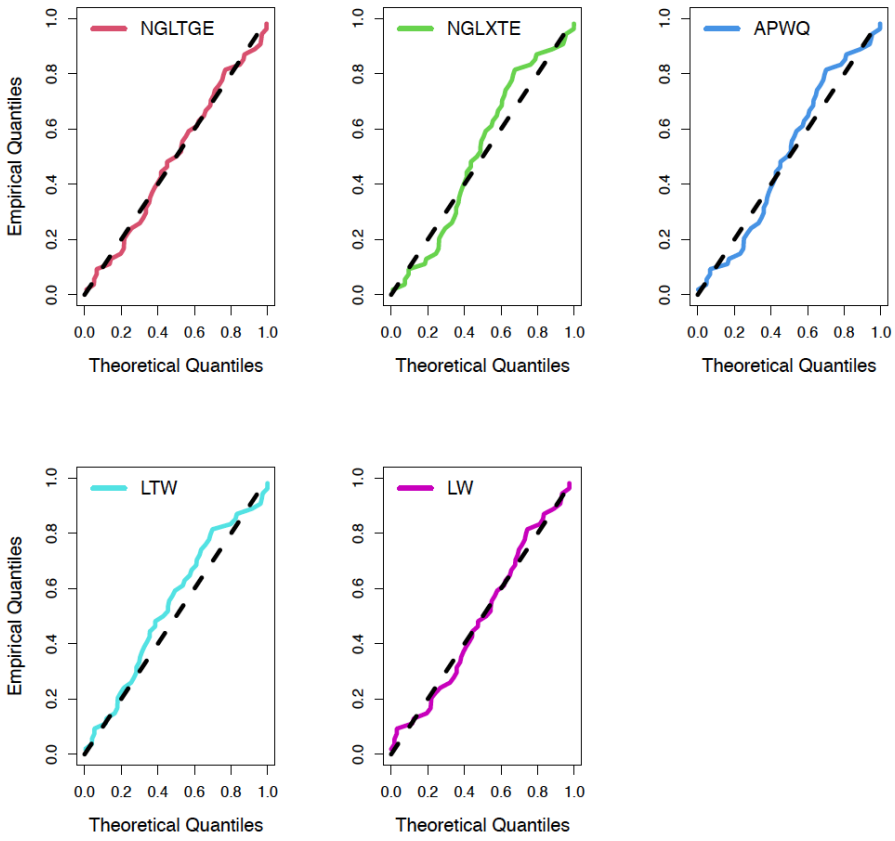


**Figure 14:** Q-Q plots for Data I.

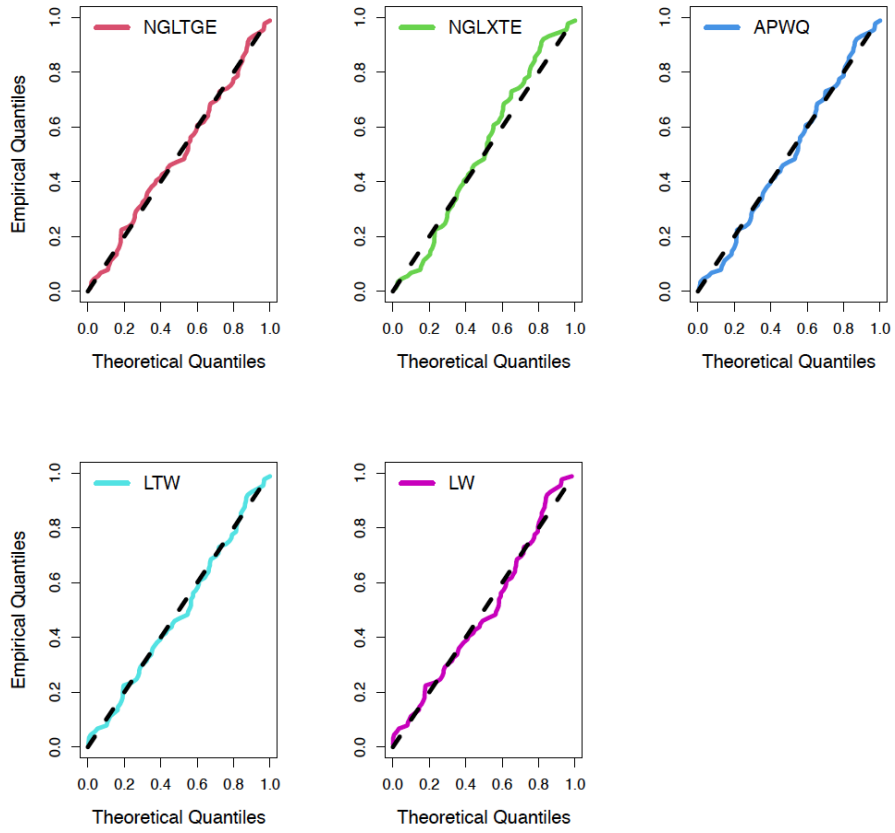


**Figure 15:** Q-Q plots for Data II.

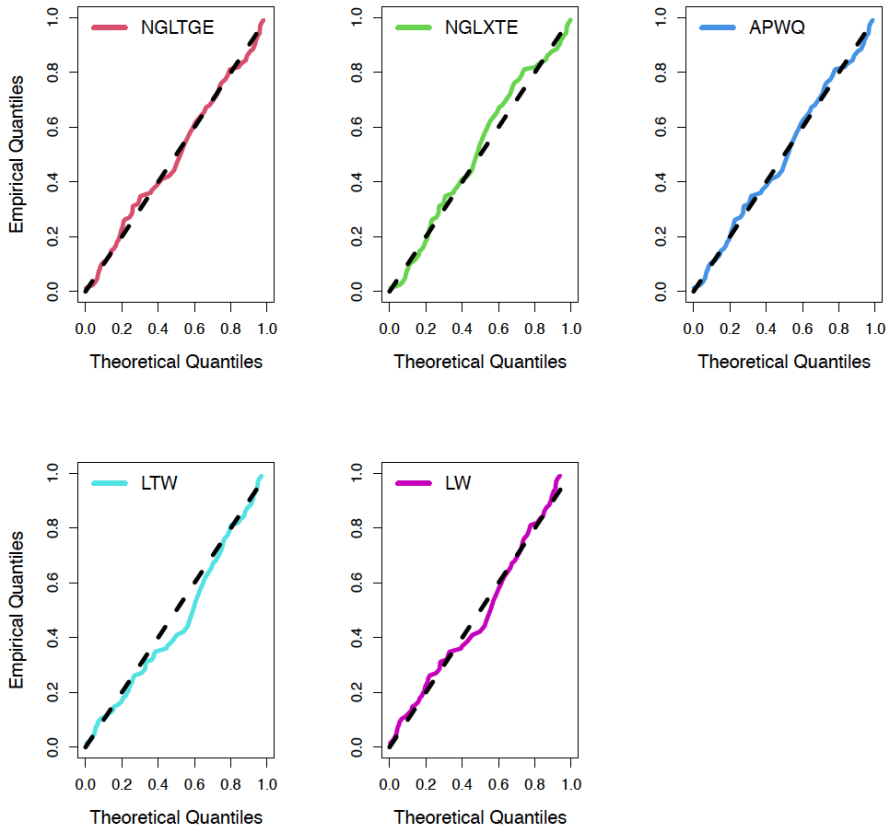


**Figure 16:** Q-Q plots for Data III.

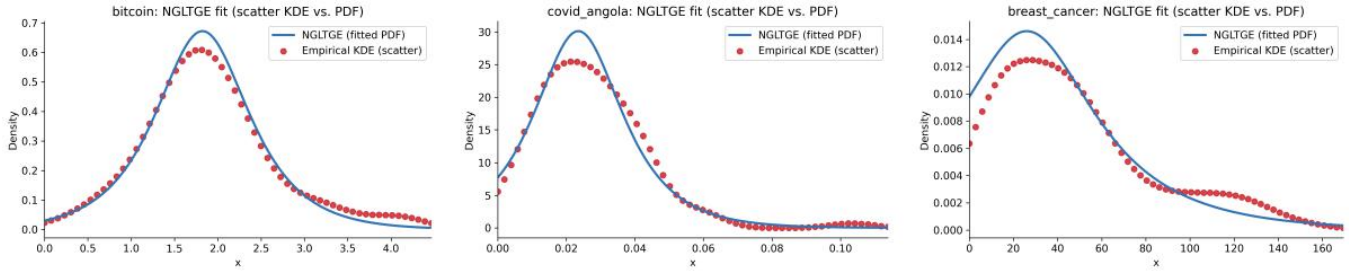


**Figure 17:** Comparison of the fitted NGLTGE PDF (blue) with empirical KDE scatter (red) for (**a**) DATA I, (**b**) DATA II, and (**c**) DATA III.

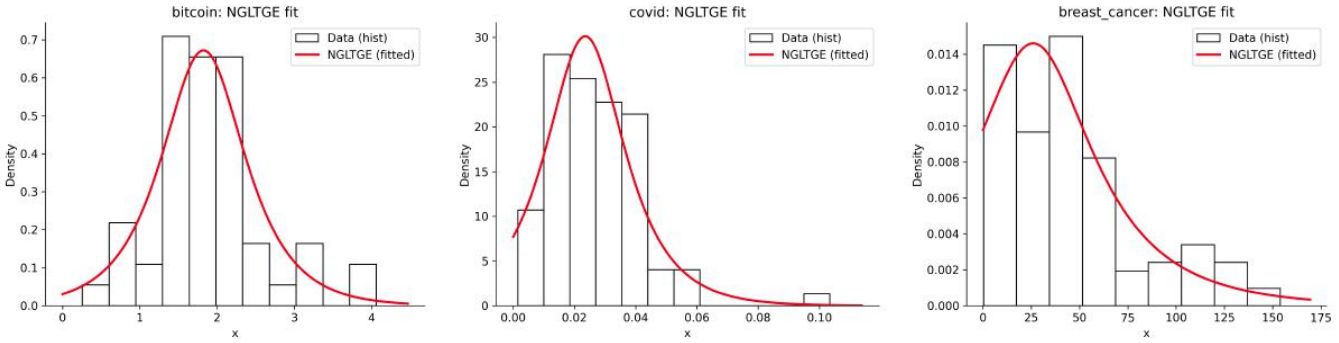


**Figure 18:** Comparison of the Fitted NGLTGE probability density functions (red curves) compared against empirical histograms (black bars with white fill) for three datasets, (**a**) DATA I, (**b**) DATA II, and (**c**) DATA III.

**Table 11: NGLTGE Parameter Estimates by Dataset. Inputs were Scaled by the Empirical 95th Percentile during Optimization; $\theta$ is on the Original Scale**

| Dataset | Init $(s_0,k_0,\theta_0)$ | $s$ (fit) | $k$ (fit) | $\theta$ (fit) |
|---|---|---|---|---|
| Bitcoin | $(0.3,1.0,0.6)$ | 0.02330 | 0.22978 | 0.47400 |
| COVID-Angola | $(0.3,1.0,0.6)$ | 0.14834 | 0.32878 | 26.8387 |
| Breast cancer | $(0.3,1.0,0.6)$ | 0.58276 | 0.38634 | 0.01019 |

monitoring held-out predictive log-likelihood using 5-fold cross-validation [47]. Adam can be replaced by a hybrid schedule (e.g., Adam warm-start followed by L-BFGS) without changing the model code. For diagnostics, we overlay the fitted PDF on data summaries using a Freedman–Diaconis histogram [48] and a kernel density estimate (KDE) [49]. This implementation integrates seamlessly with deep-learning pipelines while retaining the interpretability of a closed-form distribution.

### 8.2. Comparison with Machine Learning Density Estimators

To evaluate performance, we benchmarked NGLTGE against two state-of-the-art machine learning baselines:

1. a Log-Gaussian Mixture Model (Log-GMM), representing a flexible parametric mixture estimator in log-space [42, 50], and
2. a one-dimensional Masked Autoregressive Flow (MAF), a normalizing flow trained on $\log x$ with change-of-variables back to the original domain [44].

Predictive performance was assessed via 5-fold cross-validation of the predictive log-likelihood [47] (Table **12**, Figure **19**). Across all three real datasets-Bitcoin trading volumes, COVID-19 mortality in Angola, and breast cancer survival times-NGLTGE achieved competitive or superior performance. In particular, NGLTGE provided higher predictive log-likelihoods than both GMM and MAF in modeling heavy-tailed outcomes (e.g., survival times), highlighting its strength in domains where tail fidelity is crucial.

### 8.3. Data-Driven Validation

Beyond predictive log-likelihood, we validated model adequacy by generating synthetic datasets from the flow-based baseline [44] and visually comparing their kernel density estimates against both real data and the fitted NGLTGE PDF (Appendix A). While MAF reproduced the central modes of the distributions, it systematically underestimated tail behavior. By contrast, NGLTGE provided close alignment with empirical densities across the entire range, with fewer parameters and interpretable structure. Empirical densities were computed via kernel density estimation [49, 51-58]. This result underscores a core advantage: NGLTGE offers both statistical interpretability and ML-level competitiveness.

### 8.4. Scalability and Extensions

The computational pipeline presented here demonstrates that new distribution families can be directly embedded into modern ML frameworks [45]. Extensions such as Bayesian inference (e.g., with probabilistic programming systems) or variational inference provide posterior uncertainty quantification for $(s,k,\theta)$; in all cases, mini-batch optimization with adaptive methods like Adam [46] makes training practical at scale. Moreover, the gradient-based training opens the door to integrating NGLTGE within larger ML systems, such as survival prediction models,

**Table 12: 5-Fold Predictive Log-Likelihood (Mean ± std). Higher Values Indicate Better Generalization. Best Results for each Dataset are Shown in Bold**

| Dataset | NGLTGE | Log-GMM(3) | MAF |
|---|---|---|---|
| Bitcoin | -1.089 ± 0.208 | -1.565 ± 0.885 | -1.303 ± 0.410 |
| COVID–Angola | 2.833 ± 0.218 | 2.745 ± 0.190 | 2.675 ± 0.318 |
| Breast Cancer | -4.812 ± 0.113 | -5.112 ± 0.538 | -5.027 ± 0.241 |

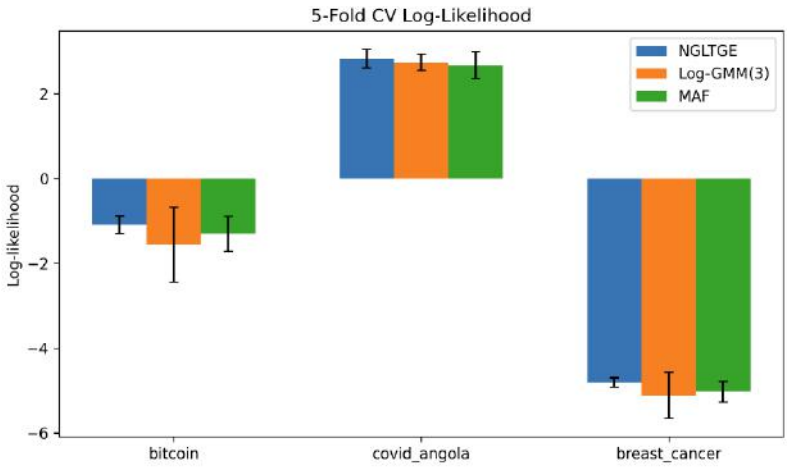


**Figure 19:** 5-fold predictive log-likelihood (mean ± std) comparison between NGLTGE, Log-GMM(3), and MAF across the three real datasets (Bitcoin trading volumes, COVID-19 mortality in Angola, and breast cancer survival times).

probabilistic forecasting pipelines, and deep generative architectures.

In summary, the ML perspective highlights that NGLTGE is not only a theoretical generalization but also a practical, scalable, and interpretable model that can compete with modern machine learning density estimators. This dual positioning strengthens its value for both the statistical and ML communities.

## 9. CONCLUSION AND FUTURE WORK

The study was successful in introducing a new family of generalized distributions, and a submodel, the new generalized Lomax tangent transformed exponential (NGLTGE) distribution. The NGLTGE distribution proved to be a more suitable model for various real datasets like cryptocurrency, COVID-19, and breast cancer data. A Monte Carlo simulation also confirmed that the parameter estimators are well-behaved asymptotically. In addition, the utility of the distribution in practice was demonstrated through its application to a group acceptance sampling plan for quality control. From a machine learning perspective, we showed that the NGLTGE model is not just an abstract concept but also an effective, scalable, and interpretable tool. By implementing it within a modern deep-learning framework like PyTorch and making use of automatic differentiation for parameter estimation, the NGLTGE distribution competed favorably with recent machine learning density estimators like Log-Gaussian Mixture Model (Log-GMM) and Masked Autoregressive Flow (MAF), particularly in the modeling of heavy-tailed data details.

The increased flexibility of the NGLTGE model, while beneficial, introduces certain practical limitations. The model has three parameters ($s,k,\theta$), making the parameter space larger and estimation more complex than the two-parameter baseline Exponential or Lomax distributions. Consequently, the Maximum Likelihood Estimation (MLE) procedure requires careful selection of initial values and can be computationally intensive for very large datasets, potentially leading to convergence issues or multiple local maxima on complex likelihood surfaces. Furthermore, while the NGLTGE excels with heavy-tailed, non-linear data, it may underperform compared to simpler models (e.g., Weibull or Gamma) when applied to data that is strictly symmetrical or possesses only very thin tails, as the added complexity becomes unnecessary overhead. Specifically, it might lack the inherent flexibility to model bi-modal or multi-modal data without further extensions, a domain where non-parametric models like Log-GMM or MAF (as shown in Section 8) often maintain an advantage.

For future work, Bayesian parameter estimation can be used to better understand the parameter uncertainty. The emphasis in the present work is on the univariate NGLTGE distribution; thus, one natural extension would be to build a multivariate counterpart to describe dependence between two or more variables and estimate it to describe dependence structures in finance and econometrics, say. While we have shown that the NGLTGE can be adapted using adaptive optimization, exploration of regularization techniques might prevent overfitting and improve generalization on small datasets. The usefulness of the NGLTGE distribution with heavy-tailed data suggests its possible application in other contexts where such features are common, e.g., network traffic simulation or actuarial science. Finally, the NGLTGE distribution could be

added to time series models or used to design new survival analysis models that can accommodate complex data.

## DATA AVAILABILITY

Data used for the study are included in this paper.

## COMPETING INTEREST

The authors declare that there is no competing interest.

## APPENDIX A: ML ESTIMATION & VALIDATION DETAILS

### A.1. Implementation

9.0.1 Kernel Density Estimation

Given samples $x_1,\ldots,x_n$, the KDE is

$$\hat{f}_h(x)=\frac{1}{nh}\sum_{i=1}^{n}K\left(\frac{x-x_i}{h}\right),$$

with Gaussian kernel $K(u)=(2\pi)^{-1/2}e^{-u^2/2}$. The bandwidth $h>0$ controls smoothness.

**Defaults.** [leftmargin=1.2em]

• Optimizer: Adam (lr $=10^{-2}$ for CV, $10^{-2}$ - $10^{-3}$ for final fits); steps $=1500$ - $2000$; mini-batch size $=32$; grad clip $=10$.

• KDE: scipy.stats.gaussian_kde (Scott's rule for bandwidth).

• Log-GMM baseline: 3 lognormal components fit on $\log x$ (sklearn GaussianMixture); prediction uses change-of-variables.

• Flow baseline (MAF): 3 affine autoregressive transforms on $\log x$ with two hidden layers (width 16), Adam lr $=5\times10^{-3}$, 1500 steps; prediction includes the $-\log x$ Jacobian term.

• Cross-validation: 5-fold, shuffled with fixed seed; we report mean $\pm$ std test log-likelihood.

### A.2. Flow Simulation

Train the flow on $y=\log x$, then sample $y^*$ from the flow and set $x^*=\exp(y^*)$. We compare $\widehat{f}_{KDE}(x)$ of the real data (solid black) against the KDE of $\{x^*\}$ (blue dashed) and the fitted NGLTGE PDF (red).

### A.3. Reproducibility

Code is written in PyTorch/NumPy; all experiments use a fixed random seed. Figures are rendered with Matplotlib; histograms use Freedman-Diaconis bins.

### A.4. Additional Figures

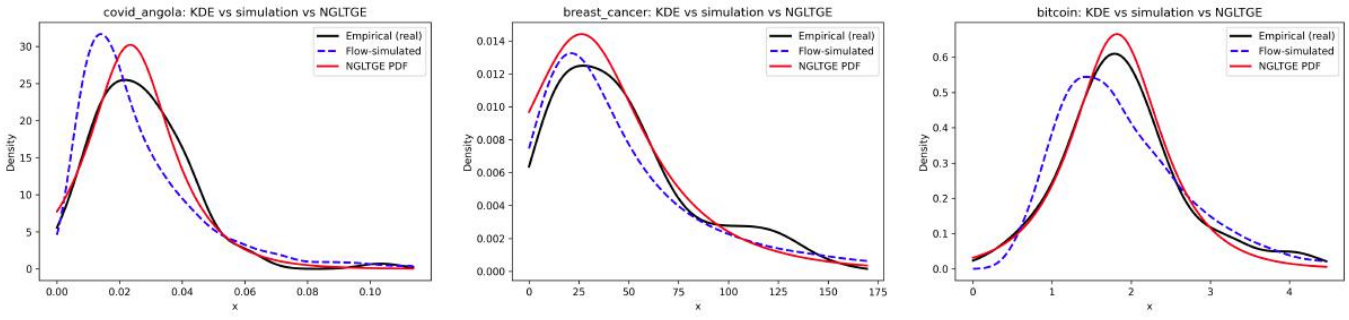


**Figure 20:** KDE overlays: empirical (black), flow-simulated(MAF) (blue dashed), NGLTGE PDF (red).

### A.5. Limitations and Future Work

[leftmargin=1.2em]

- Sensitivity to KDE bandwidth and mini-batch size; alternative optimizers or hybrid schedules.
- Tail-weighted losses and mixture-NGLTGE extensions for multi-modal data.
- Scalable Bayesian variants via stochastic variational inference (SVI).
- Covariate-dependent (conditional) NGLTGE for regression/time-varying settings.

## REFERENCES


[1] Muino JM, Voit EO, Sorribas A. GS-distributions: A new family of distributions for continuous unimodal variables. In: Computational statistics & data analysis 2006; 50(10): 2769-2798. https://doi.org/10.1016/j.csda.2005.04.016

[2] Cordeiro GM, De Castro M. A new family of generalized distributions. In: Journal of statistical computation and simulation 2011; 81(7): 883-898. https://doi.org/10.1080/00949650903530745

[3] Mehboob ZS, Sobhi MMA, El-Morshedy M, Afify AZ. A new generalized family of distributions: Properties and applications. In: Aims Math 2021; 6(1): 456-476.

[4] Benchiha SA, Sapkota LP, Al Mutairi A, Kumar V, Khashab RH, Gemeay AM, Elgarhy M, Nassr SG. A new sine family of generalized distributions: Statistical inference with applications. In: Mathematical and Computational Applications 2023; 28(4): 83. https://doi.org/10.3390/mca28040083

[5] El-Alosey AR, Alotaibi MS, Gemeay AM. A new two-parameter mixture family of generalized distributions: Statistical properties and application. In: Heliyon 2024; 10(19): https://doi.org/10.1016/j.heliyon.2024.e38198

[6] Ahmed MA, Mahmoud MR, ElSherbini EA. The new Kumaraswamy Kumaraswamy family of generalized distributions with application. In: Pakistan Journal of Statistics and Operation Research 2015; 159-180. https://doi.org/10.18187/pjsor.v11i2.969

[7] Tahir MH, Adnan Hussain M, Cordeiro GM. A new flexible generalized family for constructing many families of distributions. In: Journal of Applied Statistics 2022; 49(7): 1615-1635. https://doi.org/10.1080/02664763.2021.1874891

[8] Cordeiro GM, Ortega EMM, Ramires TG. A new generalized Weibull family of distributions: mathematical properties and applications. In: Journal of Statistical Distributions and Applications 2015; 2(1): 13. https://doi.org/10.1186/s40488-015-0036-6

[9] Bakouch H, Chesneau C, Enany M. A weighted general family of distributions: Theory and practice. In: Computational and Mathematical Methods 2021 3 (6): e1135. https://doi.org/10.1002/cmm4.1135

[10] Alzaatreh A, Lee C, Famoye F. T-normal family of distributions: a new approach to generalize the normal distribution. In: Journal of Statistical Distributions and Applications 2014; 1(1): 16. https://doi.org/10.1186/2195-5832-1-16

[11] Nofal ZM, Afify AZ, Yousof HM, Cordeiro GM. The generalized transmuted-G family of distributions. In: Communications in Statistics-Theory and Methods 2017; 46(8): 4119-4136. https://doi.org/10.1080/03610926.2015.1078478

[12] Salahuddin N, Khalil A, Mashwani WK, Shah H, Jomsri P, Panityakul T. A novel generalized family of distributions for engineering and life sciences data applications. In: Mathematical Problems in Engineering 2021; 2021(1): 9949999. https://doi.org/10.1155/2021/9949999

[13] Gemeay AM, Moakofi T, Balogun OS, Ozkan E, Md Moyazzem H. Analyzing real data by a new heavy-tailed statistical model. In: Modern Journal of Statistics 2025; 1(1): 1-24. https://doi.org/10.64389/mjs.2025.01108

[14] Mousa MN, Moshref ME, Youns N, Mansour MMM. Inference under hybrid censoring for the quadratic hazard rate model: Simulation and applications to COVID-19 mortality. In: Modern Journal of Statistics 2026; 2(1): 1-31. https://doi.org/10.64389/mjs.2026.02113

[15] Obulezi OJ. Obulezi distribution: a novel one-parameter distribution for lifetime data modeling. In: Modern Journal of Statistics 2026; 2(1): 32-74. https://doi.org/10.64389/mjs.2026.02140

[16] Onyekwere CK, Aguwa OC, Obulezi OJ. An updated lindley distribution: Properties, estimation, acceptance sampling, actuarial risk assessment and applications. In: Innovation in Statistics and Probability 2025; 1(1): 1-27. https://doi.org/10.64389/isp.2025.01103

[17] El Gazar AM, Ramadan DA, ElGarhy M, El-Desouky BS. Estimation of parameters for inverse power Ailamujia and truncated inverse power Ailamujia distributions based on progressive type-II censoring scheme. In: Innovation in Statistics and Probability 2025; 1(1): 76-87. https://doi.org/10.64389/isp.2025.01106

[18] Hassan AS, Metwally DS, Semary HE, Benchiha SA, Gemeay AM, Elgarhy M. Improved estimation based on ranked set sampling for the Chris-Jerry distribution with application to engineering data. In: Computational Journal of Mathematical and Statistical Sciences 2025. https://doi.org/10.21608/cjmss.2025.375962.1156

[19] Hassan AS, Metwally DS, Elgarhy M, Gemeay AM. A new probability continuous distribution with different estimation methods and application. In: Computational Journal of Mathematical and Statistical Sciences 2025; 4(2): 512-532. https://doi.org/10.21608/cjmss.2025.375970.1157

[20] Bousseba FZ, Zeghdoudi H, Sapkota LP, Tashkandy YA, Bakr ME, Kumar A, Gemeay AM. Novel two-parameter quadratic exponential distribution: Properties, simulation, and applications. In: Heliyon 2024; 10(19): https://doi.org/10.1016/j.heliyon.2024.e38201

[21] Alsadat N, Tanis C, Sapkota LP, Kumar A, Marzouk W, Gemeay AM. Inverse unit exponential probability distribution: Classical and Bayesian inference with applications. In: AIP Advances 2024; 14(5): https://doi.org/10.1063/5.0210828

[22] M Nassar, A Alzaatreh, O Abo-Kasem, M Mead, and M Mansoor. “A new family of generalized distributions based on alpha power transformation with application to cancer data”. In: Annals of Data Science 5.3 (2018: 421-436. https://doi.org/10.1007/s40745-018-0144-5

[23] Obulezi OJ, Obiora-Ilouno HO, Osuji GA, Kayid M, Balogun OS. A new family of generalized distributions based on logistic-x transformation: sub-model, properties and useful applications. In: Research in Statistics 2025; 3(1): 2477232. https://doi.org/10.1080/27684520.2025.2477232

[24] Zaidi SM, Mahmood Z, Nicodème MA, Tashkandy YA, Bakr ME, Almetwally EM, Hussam E, Gemeay AM, Kumar A. Lomax tangent generalized family of distributions: Characteristics, simulations, and applications on hydrological-strength data. In: Heliyon 2024; 10(12). https://doi.org/10.1016/j.heliyon.2024.e32011

[25] Gurler U. Reverse Hazard. Bilkent University, Ankara, Turkey 2016.

[26] Al-Mutairi DK, Ghitany ME, Kundu D. Inferences on stress-strength reliability from Lindley distributions. In: Communications in statistics-theory and methods 2013; 42(8): 1443-1463.

[27] Kotb MS, Raqab MZ. Inferential analysis of the stress-strength reliability for a new extended family of distributions. In: Research in Statistics 2025; 3(1): 2452926.

[28] Asgharzadeh A, Valiollahi R, Raqab MZ. Estimation of the stress-strength reliability for the generalized logistic distribution. In: Statistical Methodology 2013; 15: 73-94.

[29] Eryilmaz S. On Stress-Strength Reliability with a Time-Dependent Strength. In: Journal of Quality and Reliability Engineering 2013; 2013(1): 417818.

[30] Mokhlis NA, Ibrahim EJ, Gharieb DM. Stress- strength reliability with general form distributions. In: Communications in Statistics-Theory and Methods 2017; 46(3): 1230-1246.

[31] Cheng R, Amin N. Maximum product of spacings estimation with application to the lognormal distribution (Mathematical Report 79-1). In: Cardiff: University of Wales IST 1979.

[32] Swain JJ, Venkatraman S, Wilson JR. Least-squares estimation of distribution functions in Johnson's translation system. In: Journal of Statistical Compu- tation and Simulation 1988; 29(4): 271-297. https://doi.org/10.1080/00949658808811068

[33] Nwankwo BC, Obiora-Ilouno HO, Almulhim FA, Mustafa MSA, Obulezi OJ. Group acceptance sampling plans for type-I heavytailed exponential distribution based on truncated life tests. In: AIP Advances 2024; 14(3). https://doi.org/10.1063/5.0194258

[34] Nwankwo MP, Alsadat N, Kumar A, Bahloul MM, and Obulezi OJ. Group acceptance sampling plan based on truncated life tests for Type-I heavy-tailed Rayleigh distribution. In: Heliyon 2024; 10(19). https://doi.org/10.1016/j.heliyon.2024.e38150

[35] Ekemezie D-FN, Alghamdi FM, Aljohani HM, Riad FH, Abd El-Raouf MM, Obulezi OJ. A more flexible Lomax distribution: characterization, estimation, group acceptance sampling plan and applications. In: Alexandria Engineering Journal 2024; 109: 520-531. https://doi.org/10.1016/j.aej.2024.09.005

[36] Nadir S, Aslam M, Anyiam KE, Alshawarbeh E, Obulezi OJ. Group acceptance sampling plan based on truncated life tests for the Kumaraswamy Bell-Rayleigh distribution. In: Scientific African 2025; 27: e02537. https://doi.org/10.1016/j.sciaf.2025.e02537

[37] Lawless JF. Statistical models and methods for lifetime data. John Wiley & Sons 2011.

[38] McLachlan G, Peel D. Finite Mixture Models. Wiley 2000.

[39] Kingma DP, Welling M. Auto-Encoding Variational Bayes. In: Proceedings of the 2nd International Conference on Learning Representations (ICLR). 2014; arXiv: 1312. 6114 [stat.ML].

[40] Papamakarios G, Pavlakou T, Murray I. Masked Autoregressive Flow for Density Estimation. In: Advances in Neural Information Processing Systems 2017.

[41] Paszke A, Gross S, Massa F, Lerer A, Bradbury J, Chanan G, *et al*. PyTorch: An Imperative Style, High-Performance Deep Learning Library. In: Advances in Neural Information Processing Systems 2019.

[42] Kingma DP, Ba J. Adam: A Method for Stochastic Optimization. In: International Conference on Learning Representations 2015. arXiv: 1412.6980.

[43] Stone M. Cross-Validatory Choice and Assessment of Statistical Predictions. In: Journal of the Royal Statistical Society. Series B 1974.

[44] Freedman D, Diaconis P. On the Histogram as a Density Estimator: L2 Theory. In: Zeitschrift fÅNur Wahrscheinlichkeitstheorie und Verwandte Gebiete 1981.

[45] Silverman BW. Density Estimation for Statistics and Data Analysis. Chapman & Hall 1986.

[46] Dempster AP, Laird NM, Rubin DB. Maximum Likelihood from Incomplete Data via the EM Algorithm. In: Journal of the Royal Statistical Society. Series B 1977.

[47] Rosenblatt M. Remarks on Some Nonparametric Estimates of a Density Function. In: The Annals of Mathematical Statistics 1956.

[48] Parzen E. On Estimation of a Probability Density Function and Mode. In: The Annals of Mathematical Statistics 1962.

[49] Okechukwu CP, Asogwa EC, Aguwa OC, Obulezi OJ, Ezzeldin MR. Prediction of gender power dynamics and political representation in Nigeria using machine learning models. In: Innovation in Computer and Data Sciences 2025; 1(1): 1-18. https://doi.org/10.64389/icds.2025.01122

[50] Onyekwere CK, Nwankwo CK, Abonongo J, Asogwa EC, Shafiq A. Economic growth dynamics: a machine learning-augmented nonlinear autoregressive distributed lag model of asymmetric effect. In: Innovation in Computer and Data Sciences 2025; 1(1): 19-31. https://doi.org/10.64389/icds.2025.01125

[51] Asogwa EC, Nwankwo MP, Oguadimma EE, Okechukwu CP, Suleiman AA. Hybrid LSTM-CNN deep learning framework for stock price prediction with google stock and reddit sentiment data. In: Innovation in Computer and Data Sciences 2025; 1(1): 32-50. https://doi.org/10.64389/icds.2025.01126

[52] Nnaekwe K, Ani E, Obieke V, Okechukwu C, Usman A, Othman M. Forecasting seasonal rainfall with time series, machine learning and deep learning. In: Innovation in Computer and Data Sciences 2025; 1(1): 51-65. https://doi.org/10.64389/icds.2025.01127

[53] Ugbor G, Jamal F, Khan S, Shawki AW. Generative AI for drug discovery: Accelerating molecular design with deep learning using Nigerian local content. In: Innovation in Computer and Data Sciences 2025; 1(1): 66-77. https://doi.org/10.64389/icds.2025.01128

[54] Onyekwere CK, Nwankwo CK, Apameh DG. A hybrid machine learning framework for multi-objective performance optimization and anomaly detection in maritime operations. In: Innovation in Computer and Data Sciences 2026; 2(1): 1-10. https://doi.org/10.64389/icds.2026.02131

Received on 10-11-2025 Accepted on 15-12-2025 Published on 30-12-2025

https://doi.org/10.6000/1929-6029.2025.14.80